8-2020

Predicting Patterns of Heavy Metal Contamination in Rio Grande Valley Agricultural Soils

Joy Z. Youwakim
The University of Texas Rio Grande Valley

Recommended Citation

Youwakim, Joy Z., "Predicting Patterns of Heavy Metal Contamination in Rio Grande Valley Agricultural Soils" (2020). *Theses and Dissertations*. 796.
https://scholarworks.utrgv.edu/etd/796

PREDICTING PATTERNS OF HEAVY METAL CONTAMINATION IN RIO GRANDE VALLEY AGRICULTURAL SOILS

A Thesis

by

JOY Z. YOUWAKIM

Submitted to the Graduate College of
The University of Texas Rio Grande Valley
In partial fulfillment of the requirements for the degree of

MASTER OF SCIENCE

August 2020

Major Subject: Agricultural, Environmental, and Sustainability Sciences

PREDICTING PATTERNS OF HEAVY METAL CONTAMINATION IN RIO GRANDE VALLEY AGRICULTURAL SOILS

A Thesis
by
JOY Z. YOUWAKIM

COMMITTEE MEMBERS

Dr. Alexis Racelis
Chair of Committee

Dr. Debasish Bandyopadhyay
Committee Member

Dr. Chu-Lin Cheng
Committee Member

Dr. James Jihoon Kang
Committee Member

August 2020

ABSTRACT

Youwakim, Joy Z., Predicting Patterns of Heavy Metal Contamination in Rio Grande Valley Agricultural Soils. Master of Science (MS), August, 2020, 75 pp., 20 tables, 14 figures, references, 81 titles.

The Rio Grande Valley of Texas is the statewide leader in the production of produce and grains and is irrigated by the Rio Grande River, in which heavy metal contaminants have been documented by both the International Boundary Water Commission and the United States Geological Survey. This work attempts to observe and document patterns of heavy metal pooling in order to mitigate the increased risk of contamination due to urbanization. We hypothesize that relationships exist between heavy metal content and proximity to roads, land use, and soil type. This research tests these relationships through soil sampling and atomic absorption spectrometry (AA-S), inductively coupled plasma-mass spectrometry (ICP-MS), and portable x-ray fluorescence spectrometry (pXRF). Raw data and statistical analyses are provided for As, Cd, Cr, Cu, Fe, Ni, Pb, Se, and Zn; all samples fell under safe levels of heavy metal content provided by both the Texas Commission on Environmental Quality and the Environmental Protection Agency.

DEDICATION

First and foremost, I dedicate this thesis to my ancestors and family, without whom I would not have the motivation to conduct this work. Through countless generations of forced migration and environmental injustice, they persevered and created a safe and stable life for me to prosper in, and consequently, conduct this work. This thesis is dedicated to the ability to revolt, molt, and transform ourselves and societies into the most empowered and versatile communities equipped to alleviate the negative consequences of climate change. There is something especially beautiful about discovering aspects of ourselves that we would like to improve or change, and then having the personal will power to go about making those changes, improving our relationships with others and in turn with our Earth. It reinforces the idea that each day is a new opportunity to be an ever-evolving improved version of oneself, finding the solutions we crave to global problems, as well as the opportunity to leave this Earth in a better condition than that in which we found it. The same is true for our soils, the foundation of our food systems and webs of social connection and public health. May the information acquired through the work of this thesis serve as a tool for stewards of the Earth everywhere, especially for revolutionaries abroad who may not yet know the value of their foundational work in transforming their civil societies.

ACKNOWLEDGMENTS

This work could not have been completed without the continual support of my advisor, Dr. Alexis Racelis. I thank him for supporting my growth as a woman in STEM by believing in my ideas and agency to execute my own project, and for encouraging me to have the autonomy, responsibility, and confidence to rely on myself first and foremost as a scientist and problem solver. Whatever I needed for my work, funding, training, words of encouragement, inspiration, or a reality check, I could count on Dr. Racelis. I thank my committee members for providing me with equipment to execute my research, as well as providing me with guidance. I would next like to thank Luzyannet Ballesteros, Natalia Nevarez, and Taylor Snowden. From gathering samples to digestion analyses to late nights at the lab, thank you all for being Las Químicas Del Suelo. Many thanks to Tom Eubanks and Bryan Hoke for going out of their way to make us feel at home in 1.508 and for always being there to troubleshoot. I am thankful to all the landowners that allowed me to sample, for my time at the Texas Plant and Soil Lab, and for the relationships I created through the Center of Sustainable Agriculture and Rural Advancement. Many hugs to the agroecology lab, Nate, and Leslie, for always being there to help. Special love to Stephanie Kasper for being my rock throughout the entirety of grad school and transcending multiple dimensions of young adulthood with me, Matthew Kutugata for his acceptance of the unsolicited addition of a younger sister to his life, and Faeqa Mohsin for always saying grace. This work could also not have been possible without funding from the USDA NIFA National Needs Fellowship (#2017-38420-26758) and the National Science Foundation C-STEM Fellowship.

TABLE OF CONTENTS

LIST OF TABLES

LIST OF FIGURES

Page

CHAPTER I

INTRODUCTION

Environmental Quality in the Border Regions

The Rio Grande River spans from Southern Colorado all the way down to Texas and empties into the Gulf of Mexico and is the primary source of water for a number of municipalities, industries, and agriculture that dot the watershed. Several people cross the border every day to work in maquiladoras, which provide the added benefit of no import tax to foreign-owned countries (Wynne, 1994). Unfortunately, it has been the case historically that due to this growing industrialization of the region, wastewater finds its way into surface water and groundwater sources, polluting the Rio Grande (Wynne, 1994). A 2002 study found chemically toxic quantities of E. coli, fecal coliforms, and H.pylori in several sampling sites along the Rio Grande and attributes the source contamination to poorly maintained sewage systems, landfills, irrigation, and injection wells (Mendoza et al., 2004). While efforts have been made to ensure that treated wastewater does not get directly reused in aquaculture (Siddiqui, 2020), the same is not true for agriculture (Allende et al., 2015).

Cropland accounts for 391.5 million acres out of an estimated 1,891 million acres in the contiguous United States (USDA ERS, 2017). Urban acreage accounts for a mere 69.4M, or 3.6% of the contiguous United States, and it is estimated that 1 million additional acres a year become urban land (USDA ERS, 2017). As urban acreage increases, questions about the transformation of America’s growing spaces arise. With expansions of impervious surfaces due to roads and traffic come increases in heavy metal content in agricultural soil (Yan, 2012). Heavy metal enrichments in soil can come from a variety of other sources related to urbanization as well, such as various fertilizers, pesticides, smelting of ores, wastewater, and sewage sludge (Chen, Jing, et.al., 2018). Heavy metals most likely to be detected at contaminated sites include As, Cd, Cr, Cu, Hg, Ni, and Zn (Wuana et al., 2011). Heavy metals are associated with a variety of health concerns, such as cancer, respiratory issues, renal failure, and skin disorders (Karar et. al, 2006). Cd, Ni, and Zn are all associated with increases in car exhaust due to vehicle traffic, while As and Cd are known for the uses as pesticides and fungicides (Wuana et al., 2011; Adamiec et al., 2016). For these reasons, it is worth examining heavy metal contamination in agricultural soils as a public health concern.

Unfortunately, there do not exist many regulations for agricultural irrigation water. In 2011, the Food Safety Modernization Act (FSMA) was passed in the U.S. which advises that one sample of irrigation water be tested for E.coli and other pathogens for each water source (Allende, 2015). There is no requirement for heavy metal testing being enforced with the FSMA, as microbial pathogens are the priority (FDA, 2018). High levels of arsenic, copper, and nickel have been found in the water column and sediments of the Rio Grande in the El Paso – Juarez area (Arana, 2004) and in Laredo-Nuevo Laredo, attributed to discharged wastewater that does not meet proper environmental regulation. This is believed to be the cause of heavy metal transport to fertile soil and therefore crop contamination (Wang, 2018). This heavily affects the people living these communities, who often must make the choice between their economic and environmental health (Ramirez-Andreotta, et al., 2015). Information is increasingly available due to increased accessibility to data and testing, but of course, normal metal levels must be determined per geographic region in order to detect unusual activity. The Rio Grande Valley has a history of environmental issues not being taken care of or monitored until they are an absolute issue. For example, PCBs (polychlorinated biphenyls) were first detected in the Donna Canal in 1993, yet remediation had not been scheduled until March of 2020, which we can presume is behind schedule due to COVID-19 (EPA, 2020). Almost the same can be said for the McAllen Plume, which was first discovered in 1990 but as of 2020 is still not fully remediated, as remediation began only in 2009 (TCEQ, 2018).

Chapter one of this thesis includes a review of literature about modern, available testing, and an overview of studies that reveal reliable predictors to heavy metal in agricultural soils. A more in-depth comparison of three approaches for heavy metal characterization is presented in Chapter two, where tradeoffs in terms of accuracy, affordability, and accessibility among, AA, ICP-MS, and XRF are discussed. In chapter three, various predictors to heavy metal concentrations are explored, including distance, soil type, pH, and land use. Finally, the implications of my work are provided in the context of soils management in the RGV and other areas, with results provided to communities on their respective growing locations and how to sample themselves if they have the means.

Soil Analysis for Heavy Metals

While naturally present in soil, heavy metals can seep into our agro-ecological systems through a variety of anthropogenic source types. Through smelting, mining, agricultural chemical runoff, and mismanaged environmental dumping we see a variety of heavy metals leach into the environment. Cadmium and nickel, two weakly bonded heavy metal ions, have observed sorption behaviors on minerals and colloids that are alike in nature (Selim, 2017). Variable charge surface models as well as surface complexation models can be used to model like sorption behaviors. These types of sorption reactions can be telling of patterns within various trace elements to appear in groups or within the presence of each other (Selim, 1999). Conducting these experiments in lab to test remediation probabilities of trace elements in solution is helpful but also has limitations as sorption experiments are often not left to run as long as would be likely to happen in agricultural fields (Selim, 1999). Zinc may also be grouped with cadmium based on affinity (Selim, 2017). Competitive adsorption modeling based on the Freundlich approach leads us to the Sheindorf-Rebhun-Sheintuch approach. Using this approach, a recent study has shown that zinc in conjunction with cadmium and nickel is successful at suppression (Selim, 2017). Breakthrough curve results (BTC's) can be used to model the mobility of various contaminants as well as affinity (Selim, 2017). Single ion sorption results show that arsenic and phosphorus sorption on iron and aluminum oxides can be somewhat similar, however it is shown also that iron is more effective in adsorbing arsenic than phosphorus (Selim, 2017).

Analytical Techniques Reviewed

Today, the most respected instrument in the element composition industry is the ICP-MS. Plasma is generated from samples of almost any medium (i.e., soil, plant, water, etc.) that have undergone chemical digestion prior to being analyzed. Plasma is generated as a byproduct of the reaction of the heat of the ionization of the sample with a carrier gas, which may be Argon, Helium, or Nitrogen (Wagatsuma, 1994). Argon is used more commonly as helium is more costly, and temperatures in this process can reach up to 10,000°K (Thomas, 2008). Most recently, there is an increasing shift in the use of ICP-MS as the latest version of inductively coupled plasma spectroscopy, due to its ability to detect at low concentrations and to process results for entire element composition in one analysis (Wilschefski, 2019).

Analytical atomic absorption spectroscopy is a widely accepted tool in the field of element analysis (Lagalante, 2004). The two most commonly used methods are Graphite Furnace Atomic Absorption (GFAA) and Flame Atomic Absorption (FAA), with GFAA being the slower of the two due to the processing time (Sparks, 1996). The two-phase process involves first the conversion of an analyte molecule into its constituent gas-phase atoms (atomization), followed by the subsequent absorption of radiation of the free atoms (Lagalante, 2004). This absorption of light quantifies the concentration of elements by using either a hollow cathode lamp or an EDL to measure the amount of emission spectra produced. Temperatures in this process can range between 2300°C-2900°C, depending on if the gas used is air-acetylene or nitrous oxide acetylene, respectively (Sparks, 1996). GF-AAS and F-AAS methods are both used commonly by the EPA, and specific metals are best run on either flame or furnace, depending on anticipated metal quantity, in order to protect the graphite tube used in the GF-AAS method (Sparks, 1996).

The portable x-ray fluorescence (pXRF) is a proximal soil sensing technique (PSS) that receives much positive attention for its ability to provide a qualitative range of quick and cost-effective results (Marguí, 2007). While it is known that current models of the pXRF do not have the detection capacities of AA or ICP methods, results can sometimes be comparable (Declerq, 2019).

Non-laboratory techniques

In examining surface water runoff due to the increase of impervious surfaces, two tools used for modeling contamination of solutes are one-dimensional diffusion-wave and advection-dispersion equations (Liang, 2019). The convection-dispersion equation simulates contaminant transport in the subsurface, while advection-dispersion equations describe solute transport in overland flow (Liang, 2019). These equations can be utilized in HYDRUS-1D, a public domain software package used for modeling water flow. These are physically based models or PBMs, and once these equations are written for particular data sets, they can be the segue for machine learning techniques which can lead to various types of regressions including linear regression and the K-Nearest Neighbor regression (Liang, 2019).

In order to solve these equations, simulations using feedback neural networks or artificial neural networks can be utilized (Ghazi, 2018). These methods are becoming increasingly popular as they are quicker and more affordable than using traditional laboratory methods such as x-ray fluorescence technology (Ghazi, 2018). Hyperspectral remote sensing is becoming increasingly popular in this field for similar reasons and is a useful tool for categorizing data when it is suspected that contamination stems from one uniform source, such as mining (Lamine, 2019). Analyzing data from spectroradiometers and atomic absorption spectrometers in conjunction with remote sensing data provides for analyses of accuracy in spectral imaging as a means to advance the prevalence of heavy metal contamination work (Lamine, 2019). Using ANOVA statistical analysis, areas of overlap can be highlighted to show accuracy in using techniques such as remote sensing or neural networks in heavy metal contamination work (Lamine, 2019). The success of using remote sensing techniques can save resources like time and money research due to not having to travel to make predictions in an area that is likely to be contaminated. This can be done through the creation of soil spectral libraries, which are a way to document known spectra and contaminants in soil so that future samples can be more quickly identified (Lamine, 2019).

Chapter two examines the efficacy of three different machines' heavy metal results when presented with identical soil samples. A total of 61 agricultural soil samples taken at 7 different locational sites were analyzed for heavy metals using Inductively Coupled Plasma Mass

Spectrometry (ICP-MS) (Agilent 7500ce), Atomic Absorption Spectrometry (AAS) (PerkinElmer PinAAcle 900T), and Portable X-ray Fluorescence (pXRF) (Tracer 5g, US Analytical). Correlation between the machines varies between metal types and generally between machines, with Cr being the most consistent metal and the AA-S with the ICP-MS the most comparable analyses. Below is a map of the sampling sites used for both of these chapters.

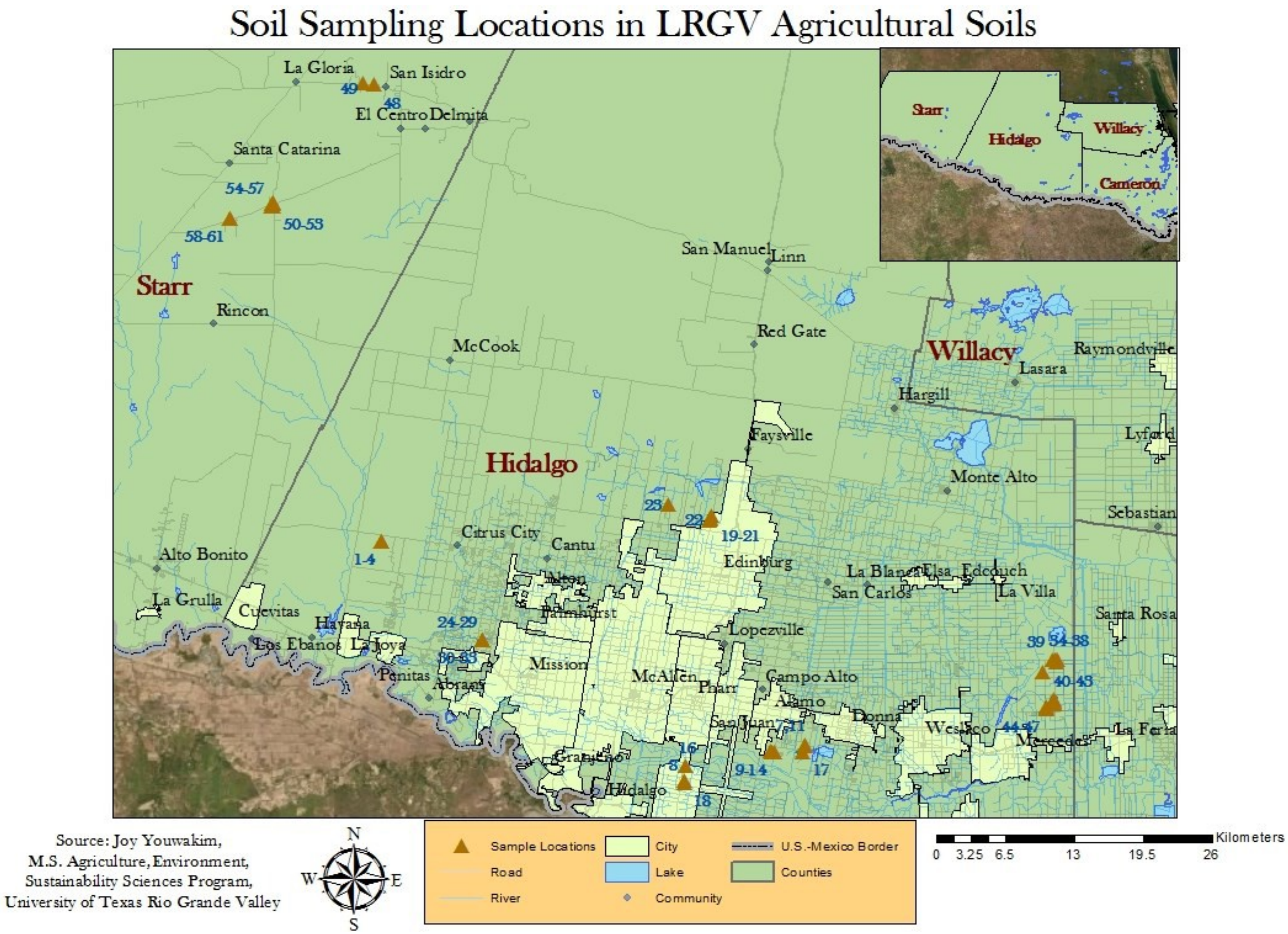

Source: Joy Youwakim,
M.S. Agriculture, Environment,
Sustainability Sciences Program,
University of Texas Rio Grande Valley

Figure 1.1 Map of Soil Sampling Locations

Predictors for Heavy Metals in Soils

Studying predictors for heavy metals provides the best advantage to preventing contamination in communities and for minimizing exposure risks, especially for field and farm workers, who are an important sector of local food systems. Heavy metal contamination is complicated as several factors can attribute to the accumulation of trace elements in soil, such as pH, organic matter, electric conductivity, and soil type (Ghazi, 2018). Ponded soils are suspect to higher rates of contamination due to improper drainage, barring any interference of infiltration rates (Yan, 2012).

Distance and Land Use

It has also been proven that roadside trees have a significant impact on heavy metal amounts in agricultural fields close to trafficked roads (Yan, 2012). In one Nepal study, measuring heavy metal uptake of plants in comparison with soils reveals that grasses have less heavy metal concentration than roadside soils (Yan, 2012). Roadside contamination from heavy metals breaks down to cadmium emissions from lubrication oil consumption and tire wear, zinc emissions from fuel tanks and tire wear, copper and lead emissions from brake wear, lead from worn metal alloys in the engine and exhaust gas from vehicles (Yan, 2012). Sample sizes for studies can vary from 30 samples to as many as 2000 depending on resources to gather on the ground data.

Soil Type and pH

Soils with higher percentages of clay and soil organic matter (SOM) are more likely to have higher heavy metal concentrations than other soil types (Dube, 2001). This can be attributed to van der Waals forces, linkage of particles through cationic bridges, i.e. Fe^{+3}, Cd^{+2}, and the cementation effects of SOM (Chessworth et. al., 2008). Lower pH levels are known to affect the bioavailability of Cd, Cu, Pb, and Zn (Chessworth et. al., 2008).

Chapter three is focused on investigative heavy metal sampling in agricultural fields and residential communities interested in farming. Environmental contamination is more likely to occur in both impoverished areas and in communities of color (Gochfield et al., 2011). The Rio Grande Valley is an at-risk area for this sort of contamination due to lax environmental regulations regarding agricultural irrigation in the United States (Allende et al., 2015). High levels of heavy metals have been detected in the Rio Grande in the Paso Del Norte Region (Rios-Arana, 2002). Due to the travel path of the river, we conducted research in the Rio Grande Valley for heavy metal contamination in agricultural fields. A total of 59 agricultural soil samples taken at 7 different locational sites were analyzed for heavy metals by Inductively Coupled Plasma Mass Spectrometry (ICP-MS). We examined and searched for heavy metal relationships by intended land use, distance from nearest road, soil type, and soil pH in order to predict patterns of heavy metal pooling due to increasing urbanization in the region. Statistical methods used for analysis include Kruskal-Wallis Rank Sum Tests and Redundancy Analyses (multivariate analysis similar to regression techniques). Results show significant differences in both Cd and Fe based on soil type. The same is true for Cu in intended land use and distance from roads. There were no significant trends or correlations based on pH, despite prior research linking it to being a very strong predictor (Zhang et al., 2018).

Heavy Metal Remediation

Remediation is one of the first topics that come to mind when we discuss heavy metal contamination and other sources of pollution. Once contamination has been detected remediation is an important consideration for habitants of nearby soil. One soil physics application is the addition of amendments which can be both organic and inorganic in nature. Organic amendments can include bark saw dust, xylogen, chitosan, bagasse, poultry manure, cattle manure, rice hulls, sewage sludge, and leaves which can immobilize various heavy metals including cadmium, lead, mercury, copper, zinc, and chromium (Wuana, 2011). Inorganic amendments include lime, phosphate salt, fly ash, slag, and bentonite which can immobilize cadmium, chromium, copper, zinc, lead, and nickel (Wuana et al., 2011). Immobilization is an applicable technique for in-situ remediation; however, the presence of bedrock or other geological formations may require ex-situ remediation (Wuana et al., 2011). Bioremediation can take several forms, including the use of phytoremediation, hyper accumulators, and in situ and ex situ remediation techniques. Hyper accumulators are plants that have the ability to remove significant amounts of heavy metals while also tolerating their presence with adequate growth (Sun et al., 2019). Phytoremediation simply refers to the usage of plants for environmental remediation (Suman et al., 2018). Some examples of plants used for hyperaccumulation are dicotyledons for cadmium and cobalt extraction, cystus ladanifer for chromium, nickel and zinc extraction, thlaspi caerulescens for cadmium and zinc extraction, arabidopsis halleri for cadmium extraction, alyssum sp. For nickel extraction, brassica junica for lead and zinc extraction, and betula, vetiveria zizaniodes and other grasses for zinc extraction (Wuana, 2011). It is important in this area of study to distinguish between geogenic and anthropogenic sources of trace elements in soil as they will vary based on geographic location (Hanesch, 2001). Monitoring environmental pollution via rock magnetic methods is a useful tool in curbing contamination, and it is known that magnetic iron oxides are able to adsorb heavy metals (Hanesch, 2001).

Summary

In an effort to bridge my interests and budding expertise in soils analysis with that of addressing pressing environmental issues, my objective was to examine and quantify heavy metals in soils of the Rio Grande Valley. The following chapters examine and compare the accuracy and accessibility of an Atomic Absorption Spectrometer, Inductively Coupled Plasma Mass Spectrometer, and a portable X-Ray Fluorescence unit. Distance, soil type, land use, and pH are tested as predictors for heavy metal concentrations in agricultural soils. It is predicted that soils that are closer to trafficked roads will exhibit higher levels of heavy metal concentration. It is also predicted that soils with higher clay content will have higher concentrations of heavy metals. Land use and pH are tested as exploratory variables, in order to see if residential areas are more susceptible to heavy metals than land intended for agricultural use.

CHAPTER II

A COMPARISON OF THREE DIFFERENT METHODS FOR THE ANALYSIS OF HEAVY METALS IN AGRICULTURAL SOIL

Abstract

Present in most soils, heavy metals are known carcinogens and harmful when ingested in excessive amounts. Testing methods and instrumentation for heavy metals in soils have improved in recent years in both efficacy and affordability. This paper examines the efficacy of three different machines' results when presented with identical samples. A total of 61 agricultural soil samples taken at 7 different locational sites were analyzed for heavy metals using Inductively Coupled Plasma Mass Spectrometry (ICP-MS) (Agilent 7500ce), Atomic Absorption Spectrometry (AA-S) (PerkinElmer PinAAcle 900T), and Portable X-ray Fluorescence (pXRF) (Tracer 5g, US Analytical). Correlation between the instrumentations varies between metal types and generally between machines, with Cr being the most consistent metal and the AA-S with the ICP-MS the most comparable analyses. Statistical analyses were performed in R Studio. These comparisons were made under the motivation that most remediation testing is not a concern of state or federal environmental agencies until it becomes a noticeable problem having already harmed existing residents. We hope this work may empower local communities to be able to test their own soils and produce if they so desire.

Introduction

Chemical characterization of soil, water, and plant material has become increasingly more available as technologies are improved and machines are optimized. Currently, there exist over a dozen techniques for element composition of soil materials. However, the tradeoffs of these differing techniques for characterization in terms of accuracy, accessibility, and dependability are more likely to be compared by machine manufacturers than by independent researchers due to restrictions such as time and cost (exceptions include the following researchers: (Pyle, 1996; Kilbride, 2006; Binstock, 2009; Radu, 2009; Declerq, 2019). Results from differing instrumentation can vary widely in efficacy, efficiency, and cost effectiveness (Pyle, 1996).

For example, many studies promote the use of Inductively Coupled Plasma –Mass Spectrometry (ICP-MS) as it purports to have the highest range of accuracy for elemental analysis (PerkinElmer, 2018; Wilschefski, 2019). However, the high cost of equipment and specialized degree of training may make the machine inaccessible to both researchers and non-researchers alike (Wilschefski, 2019). On the other hand, field-based techniques using handheld devices often used in citizen science may result in quick and real-time information, but also are somewhat rough estimates of the presence of certain elements (McComb, 2014).

These tradeoffs must be considered when addressing pressing environmental and social issues, such as remediation of heavy metals where accuracy and timeliness are equally pressing (Masten, 2016), or where results determine changes in policy and practice (Jaishankar, 2014; Ramirez-Andreotta, 2016). Furthermore, understanding of the practical and technological limitations of differing approaches must also be taken into consideration (Ramirez-

Andreotta, 2016). Although the laboratory intensive approaches may provide a higher accuracy of readings when compared to that of the use of a lower cost handheld tools, there may be situations where results may be comparable (Kim, 2019). In this work, we compare results of heavy metal analysis in three different commonly used approaches, including the ICP-MS, the AA-S, and the pXRF, across 61 different soil samples collected from various sites in south Texas. We present the results and discuss the tradeoffs of each approach as it pertains to accuracy, precision, and accessibility.

Methods of Element Composition

One of the most highly regarded techniques for soil element quantification is inductively coupled plasma spectroscopy (ICP), where plasma is generated from samples of almost any medium (i.e., soil, plant, water, etc.) that have undergone chemical digestion prior to being analyzed. Plasma is generated as a byproduct of the reaction of the heat of the ionization of the sample with a carrier gas, which may be Argon, Helium, or Nitrogen (Wagatsuma, 1994). Argon is used more commonly as helium is more costly, and temperatures in this process can reach up to 10,000°K (Thomas, 2008). The more affordable form of Inductively Coupled Plasma analysis includes optical emission spectroscopy (ICP-OES) or atomic emission spectroscopy (ICP-AES) (Wilschefski, 2019). Most recently, there is an increasing shift in the use of ICP-MS as the latest version of inductively coupled plasma spectroscopy, due to its ability to detect at low concentrations and to process results for entire element composition in one analysis (Wilschefski, 2019).

The first analytical atomic absorption spectrophotometer (AA-S) was created by Alan Walsh in 1953 and has become a widely accepted tool in the field of element analysis ever since

(Lagalante, 2004). The two-phase process involves first the conversion of an analyte molecule into its constituent gas-phase atoms (atomization), followed by the subsequent absorption of radiation of the free atoms (Lagalante, 2004). This absorption of light quantifies the concentration of elements by using either a hollow cathode lamp or an EDL to measure the amount of emission spectra produced. Temperatures in this process can range between 2300°C-2900°C, depending on if the gas used is air-acetylene or nitrous oxide acetylene, respectively (Sparks, 1996). The two most commonly used methods are Graphite Furnace Atomic Absorption (GFAA) and Flame Atomic Absorption (FAA), with GFAA being the slower of the two due to the processing time, as it is capable of analyzing only one element at a time with specified lamps (Sparks, 1996; PerkimElmer 2011). GF-AAS is used to detect metals with expected lower concentrations compared to F-AAS which should be reserved for more major elements to protect machine equipment (Wilson, 2008). Not all researchers may have access to a model with both a flame and a furnace, in which case, sensitive metals may be run on an ICP if available. The advantages of an AA-S are that it takes less training than an ICP to operate and can be faster than ICP if the concern is single element (Wilschefski, 2019). Please see Table 1 for minimum detection limits.

The portable x-ray fluorescence (pXRF) is a proximal soil sensing technique (PSS) that receives much positive attention for its ability to provide a qualitative range of quick and cost-effective results (Marguí, 2007). While it is known that current models of the pXRF do not have the detection capacities of AA or ICP methods, results can sometimes be comparable (Declerq, 2019). As a more commonly accepted alternative to traditional laboratory testing, enhanced usage of pXRF mechanisms may assist in the discovery of potentially contaminated sites more quickly than analyses requiring digestion, however it is still emphasized by some (Ridings, 2000) that pXRF technologies are not reliable enough to fulfill this role, as reviewed by (Lemière, 2018). The pXRF functions through the emission of spectra by beaming x-rays at samples (Marguí, 2007). The machine then reads the spectra to provide element quantification. For the use of heavy metal analyses, one limit can be quantification, as most models of pXRF provide semi-quantitative analyses, which can be transformed through softwares like ArTax or EasyCal (Bruker, 2020). Traditionally the pXRF is used for elements lighter than heavy metals, with heavy metal and nutrient calibrations being added with the latest models of the Tracer series (Bruker, 2020).

More recently, interpolation methods are being utilized such as kriging and inverse distance weighing that apply fluorescence and geographic information systems to characterize soils (Kim, 2019). Approaches like this can save time and money used for materials and labor when making predictions about areas of contamination. Other tactics used include partial differential equations and artificial neural networks that function as feedback neural networks (Ghazi, 2018). Remote sensing is also a growing tactic in spatial analysis, and researchers are proving the validity of these methods by coupling their mappings with in-lab results, in one case with a spectroradiometer (Lamine, 2019). These techniques reduce the need for chemistry laboratories and the use of chemicals and have been deployed in various settings including mining and land use planning, when coupled with unmanned aerial vehicles (Lamine, 2019).

This paper analyzes the efficacy of three of the more common techniques used across labs: the Inductively Coupled Plasma Mass Spectrometer (ICP-MS), the Atomic Absorption Spectrometer (AA-S), and the Portable X-ray Fluorescence (pXRF). Comparative studies have revealed specific differences among these machines when it comes to costs, efficiency, error, and accuracy (Pyle, 1996; Kilbride, 2006; Binstock, 2009; Radu, 2009; McComb, 2014; Hu 2014). Both Hu and Radu advocate for the speed of the pXRF in providing contamination results and present strong correlation coefficients for results when compared to both ICP-MS and AA methods (Radu, 2009; Hu, 2014). Binstock et al found that the FPXRF was a reliable tool when it came to detection of lead (Pb) in residential soils (Binstock, 2009). A study done on South Korean beaches found that the use of pXRF in sandy soils was highly accurate in comparison to results from the ICP (Kim, 2019). Some argue that through the partial digestion process, an accurate reading of the metal content is more challenging to obtain when compared to the capability of the pXRF to take a read from the entire soil sample (Kilbride, 2006). We add to this literature by using the same set of samples to compare the results from these techniques.

Methods

Sample Collection and Preparation

For this comparative study, we used 61 composite soil samples collected using step-down soil corers (AMS, city, state), gathering soil samples at depths of no greater than 30cm. Samples were collected in 2019 as part of another study (Youwakim, unpublished (see chapter III), and ranged from a variety of soil types and uses. Samples were numbered and stored in laboratory conditions until processing and digestion. Samples were read on an Inductively Coupled Plasma Mass Spectrometer (Agilent 7500ce), Atomic Absorption Spectrometer (PerkinElmer PinAAcle 900T), and Portable X-ray Fluorescence Gun (Tracer 5g, US Analytical). The digestion method was utilized only for the ICP-MS and both the GFAA and the FAA. Samples for the pXRF were read both as they came from the field and after the initial drying preparation step. Preparation for this included filling polyethylene sample cups with thin film for both the wet and dry samples. Samples were dried for 12 hours at 91 degrees C in a gravimetric oven (Lindberg blue). Samples were ground by hand in mortar and pestles and then sieved to 2mm.

Sample Digestion

Soil digestion required for analysis with the AA-S and ICP-MS was performed using EPA method 3050B, with slight modifications outlined below and as described in Test Methods for the Examination of Compost and Composting (U.S. Composting Council, 2002). Similar methods have been used for digestion in both agricultural and marine sediments (Peña-Icart, 2011).

1-gram samples of sieved soil were then weighed out in 2.5 x 20cm test tubes. 10mL of 35% nitric acid (HNO_3) were added to each sample in a test tube digestion block (SPB 50-24 PerkinElmer). Samples were then refluxed for 15 minutes at 95°C. Another 5 mL of 35% nitric acid (HNO_3) were then added and the samples were refluxed for another 30 minutes. Then, 3mL of 37% hydrochloric acid (HCl) were added and samples were heated at one hour in the test tube block, still at 95°C. After this step, the digestion block temperature was lowered to 80°C. 3 mL of 30% hydrogen peroxide (H_2O_2) were added with a 5 minute resting period before adding an additional 1mL of H_2O_2 with 5 min intervals until no more than 10mL of hydrogen peroxide (H_2O_2) were added (in order to avoid bubbling over and losing sample). If a drop was added and there was no reaction, the participant could stop adding hydrogen peroxide, however, this did not occur with any of our samples. The digestion block temperature was then raised again to 95°C before adding 10mL of deionized water. Samples were then refluxed for 15 min at 95°C. The digestion block was then turned off and samples were diluted with deionized water in 100mL volumetric flasks. Samples were stored at room temperature until processed using the different methods described below.

Sample Processing

Inductively Coupled Plasma Mass Spectrometer

Samples for the ICP-Q-MS (Agilent 7500ce) analysis were run at the University of Texas at Austin at the Jackson School of Geosciences in the ICP-Q-MS lab (Dr. Nathan Miller). Samples were diluted by a factor of 25 in a medium of 2% nitric acid (HNO_3). A semi-quantitative analysis was run initially before running a full quantitative analysis. All lab materials were sterilized in 2% nitric acid (HNO_3). ICP-MS analytical parameters are shown in Tables 2 and 3.

Cation concentrations (Li, B, Na, Mg, Al, Si, P, K, Ca, Ti, V, Cr, Mn, Fe, Co, Ni, Cu, Zn, As, Se, Rb, Sr, Zr, Mo, Ag, Cd, Sn, Sb, Cs, Ba, Tl, Pb, Bi, Th, and U) were determined using an Agilent 7500ce ICP-MS. The instrument was optimized for sensitivity across the AMU range, while minimizing oxide production (< 1.4%). Because of uncertainty related to elemental concentrations and matrix compatibilities for initial digests, samples were first analyzed semi-quantitatively in helium collision mode (Wilbur, 2007), then quantitatively after 25x further dilution. The quantitative analytical method employed an octopol reaction system (ORS), operated in helium (collision-mode) and hydrogen (reaction-mode) for removal of polyatomic interferences. Internal standards, mixed into unknowns via in-run pumping, were used to compensate for instrumental drift and internal standard sensitivity variations were well within QA tolerances (± 50%). Limits of detection based upon the population of blank (2% HNO_3) analyses interspersed throughout the analytical sequence were typically better than 0.670 ppb (median = 0.019 ppb) for analytes measured in optimal modes (with or without the ORS). Limits of detection excluding the following major elements Na, Ca, Mg, K, P, Al, Fe, read with an average of (0.080 ppb; median 0.009 ppb). Analyte recoveries obtained for replicates of two independent quality control standards ranged between 96 to 100% of certified values. Relative precisions (n = 2-7) obtained for these quality control standards were typically within 0.0 to 4.0 % of replicate 3.952e-11 averages. Minimum detection limits and recoveries for elements of importance can be found in Table 5.

Atomic Absorption Spectrometer

For the AA-S (PerkinElmer PinAAcle 900T) analysis, all samples were read in duplicate. Standards were made in a medium of 5% nitric acid (HNO_3). Both hollow cathode and electrode-less discharge lamps (EDL) were used for various metals. Samples with a relative standard deviation (RSD) above 20% were run again. Standards for each sample were made after the results from the ICP-MS were complete. Aliquot volume was 20 microliters for each sample. For metals that needed a matrix modifier, 5 microliters of modifier were added to 15 microliters of sample. Zn and Fe were run via FAA, while As, Cd, Cr, Cu, Ni, Pb, and Se were run via GFAA. Quality was assured through calibration coefficients detailed in Table 4.

Portable X-ray Fluorescence Gun (Tracer 5g, US Analytical)

The samples that were run for this study were run using a handheld PXRF. The instrument uses a Rhodium X-ray tube operated at 40 KeV in the *nutrients and heavy metals in soil* calibration using sharp beam technology. Sharp beam is a patented collimator system optimizes the front-end geometry of the tube and detector. This places the X-ray source as close to the sample as possible. This results in a higher intensity being able to reach the sample per unit current to the tube. Quantification of elements is accomplished using an ultra-high resolution (<140 eV at 250,000 count per second Mn Kα) silicon drift detector. The window of the detector is made of graphene compared to traditional PXRF units that use beryllium as the detector window. The graphene window is an advanced material composed of atomic layers of carbon atoms arranged in hexagonal lattices. The graphene allows for a higher transmission of X-rays throughout the energy spectrum, which dramatically improves the transmission for light elements. Samples were scanned through the 8mm aperture sequentially for 60 seconds per beam, with one complete scan being 120 seconds. Data quality was verified using a certified USGS standard SdAR-M2 metal rich sediment check sample at beginning and end of scanning. pXRF results were reported by the instrument in weight percent. These values were converted to ppb by multiplying first by 10,000 to reach ppm and then by another 1000 to reach ppb. Then these numbers were divided by 100 in order to convert from µg/kg to µg/l in order to compare between ICP-MS and AA data. These converted numbers are reported in the appendix.

Figure 2.1 Tracer 5g at UTRGV

Results

The Spearman's Rank Correlation method was used due to data that could not be normalized. Respective rho values reveal a consistency among Cr for high correlation between each machine and its counterpart. A table with averages and correlation coefficients is shown in Table 6, along with scatterplot matrices for each metal with each of the three machines (appendix 1). Correlations between wet and dry pXRF data produced identical rho values. Reasons to describe discrepancies between machine readings include variances in operating users, machine settings, and physical lab location and subsequent procedures, along with non-identical limits of detection per machine. There exist statistically significant relationships between a majority of tested elements and their respective machines. All statistical analyses were executed in R Studio software.

Discussion

Both very strong significant and very strong positive correlations exist between the ICP and AA for Cr, Cu, and Pb. These are followed by a series of strong positive correlations with very strong significance for Fe and Ni between the ICP and AA, for As, Cr, and Zn between the AA and pXRF, and for Cd, Cr, Fe, and Ni between the ICP and pXRF. Lastly, there exist a series of moderate positive correlations that are also very significant for Cd between the ICP and AA, for Fe, Ni, and Pb between the AA and pXRF, and for Pb and Se between the ICP and pXRF.

Our purpose for testing these same 61 samples on 3 different machines was to compare the efficacy in data analysis to provide a margin of error estimate for universities unable to purchase an ICP-MS or ICP-Q-MS, or even an Atomic Absorption Spectrometer. While this research focuses on comparing nine metals of interest, it is often the case in contamination investigations that only one or two metals are of focus. We hope that the data provided may assist users in choosing which machine is most equipped to handle their investigative needs. Different standard solutions were used on the ICP-MS and AA-S as they were run in different laboratory settings.

In terms of speed, the FAA provided the shortest analysis time, followed by the pXRF, then the ICP-MS, and lastly the GFAA. While the ICP-MS is the most expensive piece of equipment, we assume it also provides the most accurate results (Wilschefski, 2019). The AA is perhaps a common middle ground, as a piece of equipment less expensive than the ICP but with higher accuracy rates than the pXRF. The pXRF consistently overestimated for every metal except for Fe. This work does not aim to discredit the reliability of the pXRF, as we can see it trends accurately, but aims to point out the inexact measurements provided by the machine when compared to more traditional laboratory techniques for element composition.

Between these three machines there are differences in reported levels of element composition. Several factors can be the cause of this including user error, machine sensitivity, detection limits, inconsistency in users, and variation in temperature and storing conditions. This is important to note as it is unlikely for a researcher or concerned citizen to have access to all the machines at once that this study utilizes, and to consider when sending samples to various labs and analyzing discrepancies. For the pXRF it is often mentioned that dried and sieved in lab samples read more accurately than wet or in field samples, but upon our analysis the correlations were identical. All raw data can be found in the appendix. For researchers that do not have access to ICP-MS, and perhaps only have access to devices like the pXRF, the discussion of precision when reporting contamination numbers is likely to come up.

Contamination levels vary between countries and their respective states and provinces, however, in the U.S. the numbers are lax enough that our large pXRF readings still do not come close to any of the limits provided by the EPA or TCEQ. If researchers are concerned about accuracy but limited by cost, it may be best to use the pXRF to first check for the possibility of contamination in their region, and then to pay for an ICP or AA analysis for further certainty. See Table 7 for a summary of advantages and disadvantages for these three machines.

Acknowledgements

In no way does this work endorse the purchase of any of the above machines. Bruker Analytical granted us the use of the Tracer 5g pXRF. The ICP-MS Lab at UT Austin collaborated with us to test our samples on the ICP-MS. This graduate work was funded by the USDA-NIFA National Needs Fellowship program (grant number: #2017-38420-26758).

Tables and Figures

Table 2.1. Instrument Minimum Detection Limits in micrograms per liter (µg/L) or (ppb)

Element	FAA	GFAA	ICP-MS	pXRF
As	150	0.05	0.0003	50
Cd	.8	0.002	0.00006	200
Cr	3	0.004	0.00005	50
Cu	1.5	0.014	0.00003	<50
Fe	5	0.06	0.0001	150
Ni	6	0.07	0.00006	50
Pb	15	0.05	0.00001	90
Se	100	0.05	0.0003	<50
Zn	1.5	0.02	0.0001	<50

Table adapted from (PerkinElmer, 2018) and (Bruker, 2018)

Table 2.2 Semi-quant analyses in He mode on 10/17/19

Mode	Rate
Ar Carrier	.7L/min
Ar Makeup	.42L/min
He Mode	5.5mL/min
H2 Mode	NA

Table 2.3. Quantitative analyses in no gas, He- and H2-modes on 10/18-19/19

Mode	Rate
Ar Carrier	0.7L/min
Ar Makeup	0.49L/min
He Mode	4.3mL/min
H2 Mode	3.7mL/min

TABLE 2.4 CONDITIONS USED DURING GFAA ANALYSIS

SETTING	ELEMENT						
	As	*Cd*	*Cr*	*Cu*	*Ni*	*Pb*	*Se*
WAVELENGTH RECOMMENDED (NM)	193.7	228.8	357.87	324.75	232	283.31	196.03
LAMP READINGS SIGNAL	63	68	99	84	57	78	63
SLIT WIDTH (NM)	0.7	0.7	0.7	0.7	0.2	0.7	2
MATRIX MODIFIER RECOMMENDED	0.005mg Pd+0.003mg Mg(NO3)2	0.015mg Mg(NO3)2	0.015mg Mg (NO3)2	0.005mg Pd +0.003mg Mg (NO3)2	N/A	0.05mg NH4H2PO4 + 0.003mg Mg (NO3)2	0.005mg Pd +0.003mg Mg (NO3)2
USED MATRIX MODIFIER	Yes	Yes	No	No	N/A	Yes	No
PYROLYSIS TEMPERATURE RECOMMENDED(◦C)	1200	500	1500	1200	1100	850	1300
PYROLYSIS TEMPERATURE USED(◦C)	1200	1000	1500	1200	1100	850	1300
ATOMIZATION TEMPERATURE RECOMMENDED (◦C)	2000	1500	2300	2000	2300	1600	1900
ATOMIZATION TEMPERATURE USED (◦C)	2000	2200	2300	2000	2300	1600	1900
CALIBRATION METHOD	Non-linear through zero	Non-linear through zero	Linear through zero	Non-linear through zero	Non-linear through zero	Non-linear through zero	Non-linear through zero
CALIBRATION CORRELATION COEFFICIENT	0.999991	1	0.974776	0.998683	0.995961	1	0.999706

Table 2.5 Analytical Data for ICP-MS Agilent 7500ce During Analysis in PPB

					Element				
Type	**As**	**Cd**	**Cr**	**Cu**	**Fe**	**Ni**	**Pb**	**Se**	**Zn**
MDL	.9	0.075	0.225	0.2	46.325	.15	0.1	0.8	7.4
Recoveries	.94-.96	.89-.92	.99-1.01	.98-1.01	.99-1.04	.97-1.01	.98-1.02	.96-1.03	.99-1.04
QC 1 StDev	.168	.091	.900	.021	.148	.007	.064	.484	.042
QC 2 StDev	.288	.197	.239	.339	1.29	.307	.393	.311	1.619
QC 3 StDev	.317	.015	.044	.064	.233	.159	.072	.088	.215
LOD	.045	.003	.009	.008	1.853	.006	.004	.032	.276

Table 2.6 Samples Averages Between Metal and Instrument (ppb)

	Element (*-Flame)								
	As	Cd	Cr	Cu	**Fe***	Ni	Pb	Se	**Zn***
ICP-MS	15.26	3.13	100.76	134.66	95453.43	103.97	87.02	1.39	1940.48
AA	57.90	0.30	106.32	78.08	109804.9	126.20	97.77	2.58	850.36
pXRF	56.39	133.11	57.54	52.79	170.66	78.20	46.23	24.92	45.74
Spearman's Rank Correlation Rhos between Metal and Machine Type									
ICP x AA	-0.187	0.433***	0.951***	0.871***	0.701***	0.751***	0.929***	0.182	.125
AA x pXRF	0.689***	0.322*	0.776***	0.272*	0.454***	0.595***	0.536***	0.092	0.621***
ICP x pXRF	-0.025	0.725***	0.797***	0.175	0.745***	0.735***	0.454***	0.493***	0.063

*p<0.05, **p <0.01, ***p<0.001

Table 2.7. Capabilities and Limitations of ICP-MS, GFAA, FAA, and pXRF

Instrument	Capabilities	Limitations	Average Cost in USD
ICP-MS	Able to run with low sample volume, able to process multi-element requests, lowest of the detection limits, able to process several samples in a short amount of time, can execute sample analysis without supervision	High upfront cost, high costs of maintenance, careful digestion method required, high level of training required.	170,000-350,000
GFAA	Low detection limit, may be left unattended in most cases, low sample volume needed, accessible price and camera available to aid in troubleshooting	Single element analysis, highly time consuming for multi-element inquiries	50,000-70,000
FAA	3-4 second reading time, high sample output, low training requirements, most affordable in-lab-only technique.	Single element analysis, can take up to approximately 8mL to run each sample in triplicate, High detection limit, requires constant attention if there is no autosampler.	30,000-50,000
pXRF	Low operating costs, 60 second reading time, affordable, requires little training to operate, Multi-element analysis can be taken to the field for instant readings.	High detection limit, inaccurate readings common when reading for metals in low quantities.	40,000-60,000

(Bruker, personal communication, 2020), (Wilschefski, 2019), (PerkinElmer, personal communication 2020), (PerkinElmer, 2018).

Data Analysis Figures 2.2-2.10 (All units in ppb, µg/l)

The following matrices provide visual illustrations of the correlation between concentrations. Axes correspond to the respective data for each instrument.

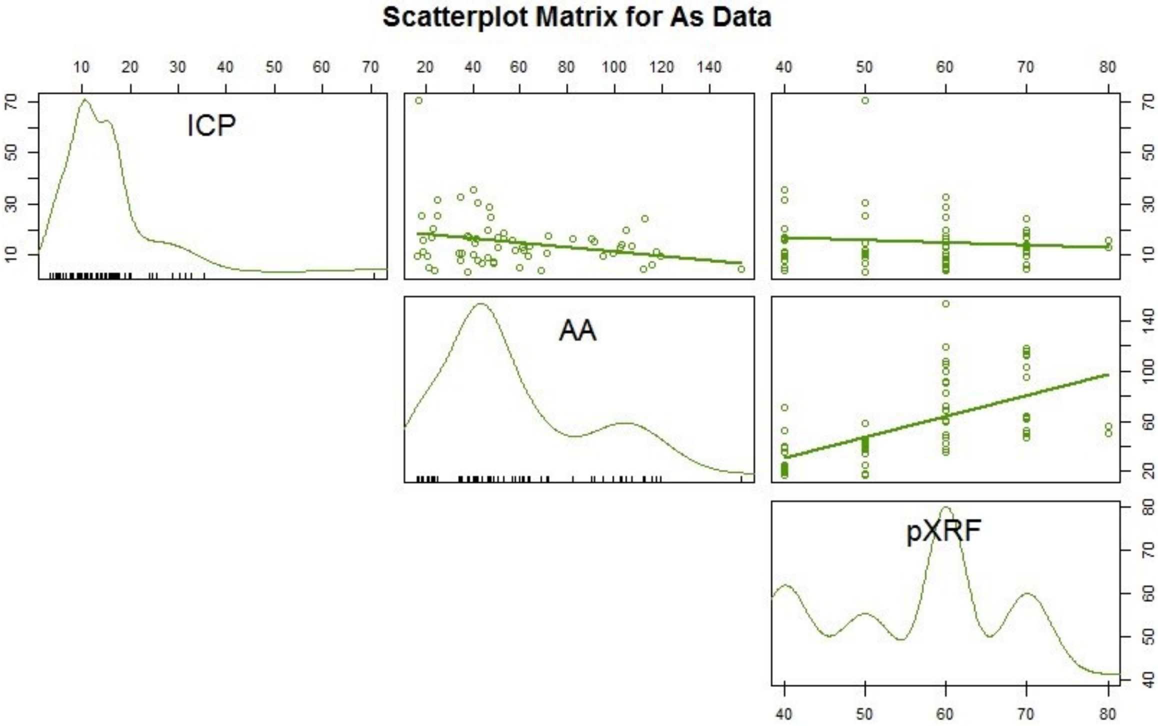

Figure 2.2 Scatterplot Matrix for As Data

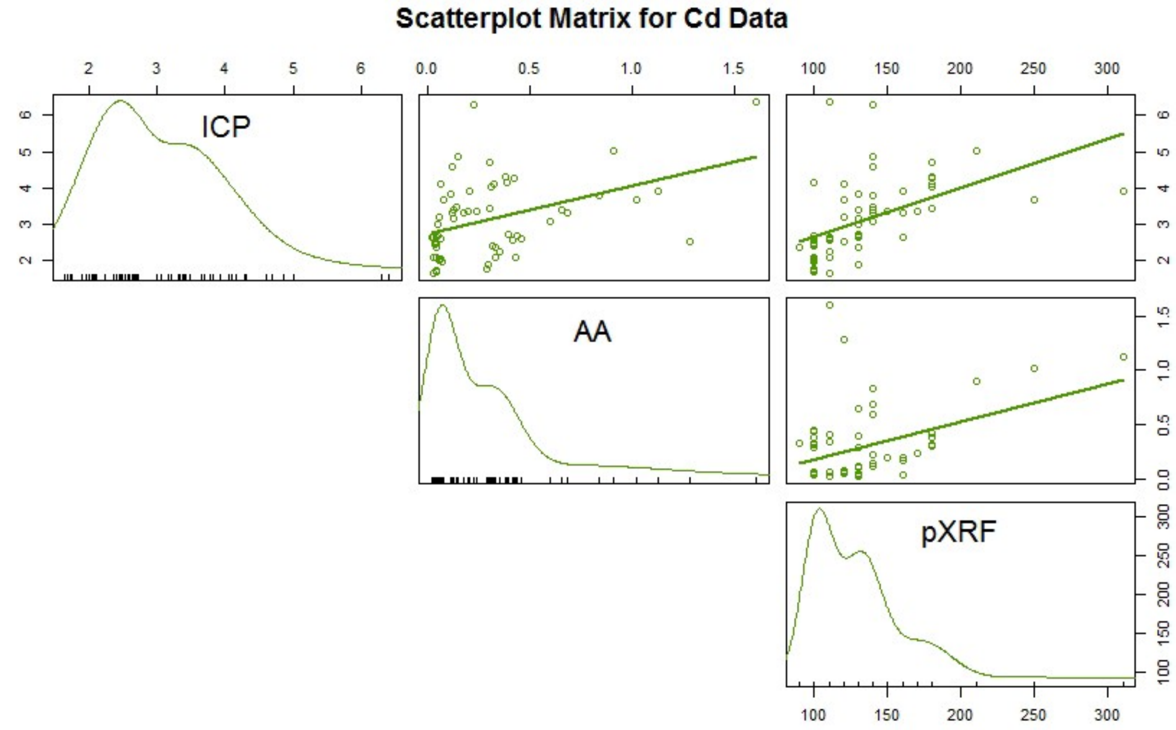

Figure 2.3 Scatterplot Matrix for Cd Data

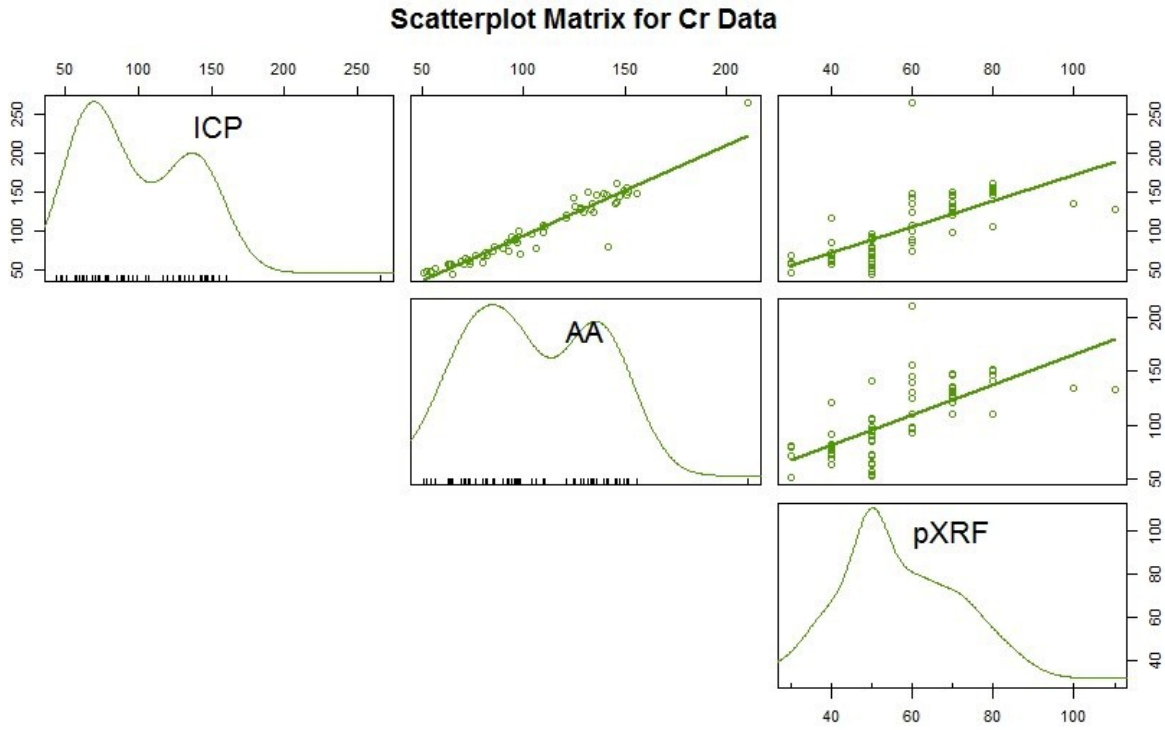

Figure 2.4 Scatterplot Matrix for Cr Data

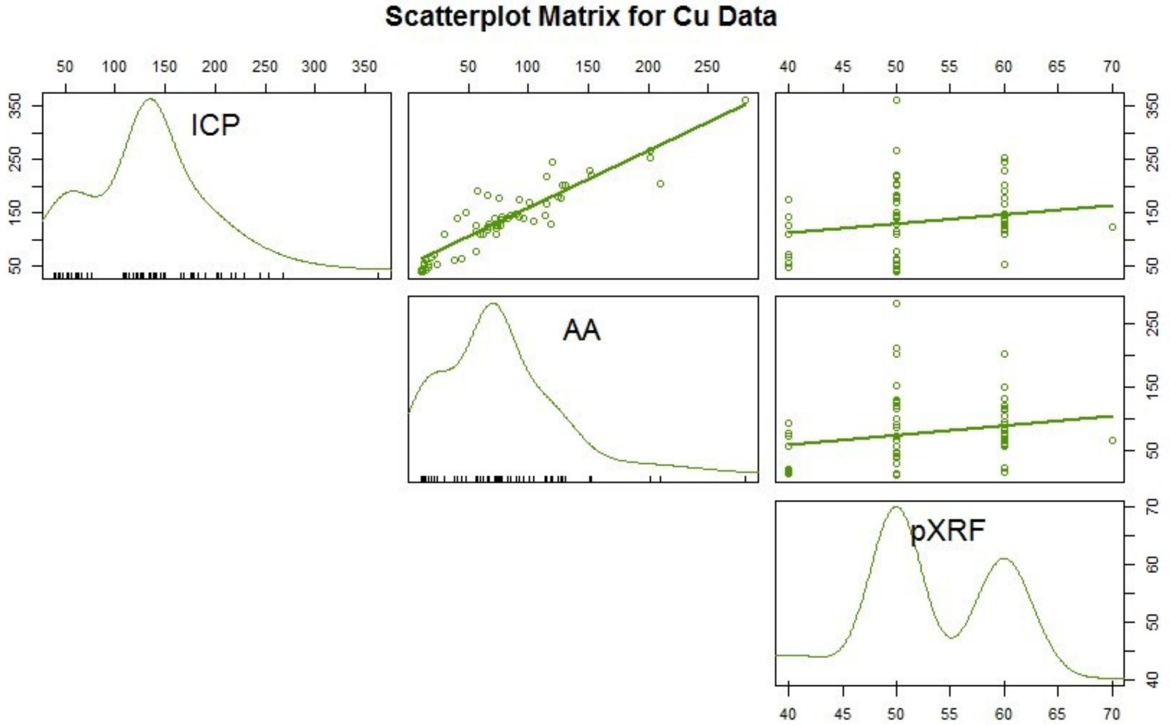

Figure 2.5 Scatterplot Matrix for Cu Data

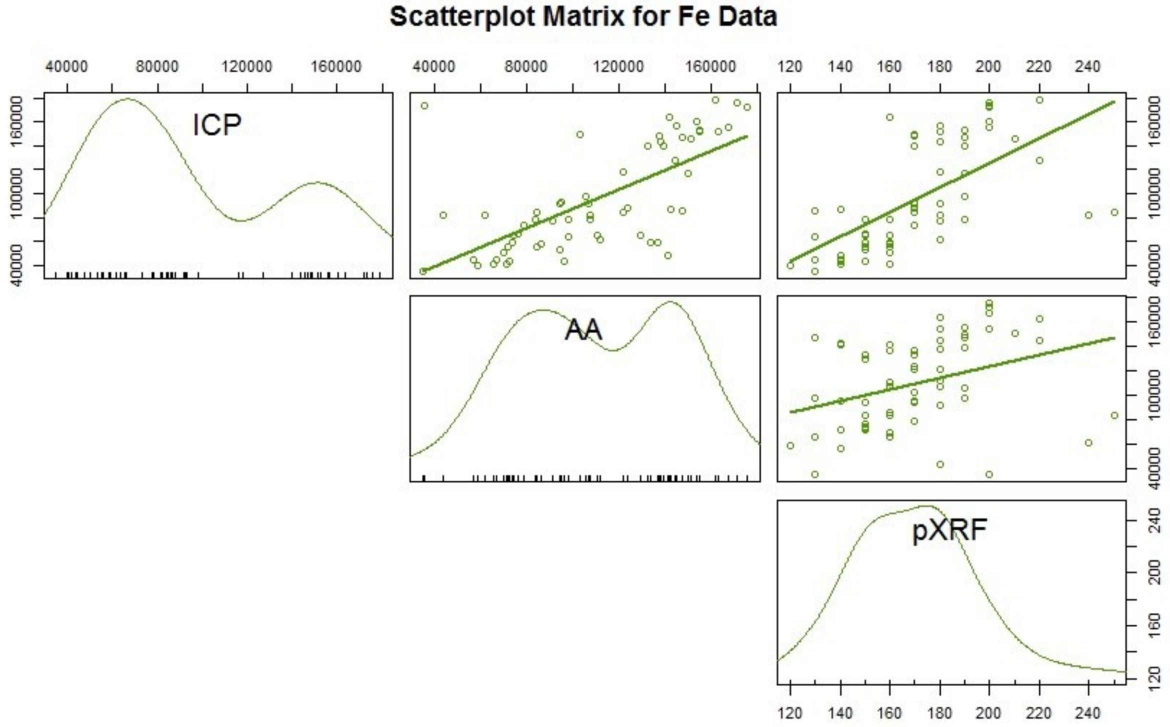

Figure 2.6 Scatterplot Matrix for Fe Data

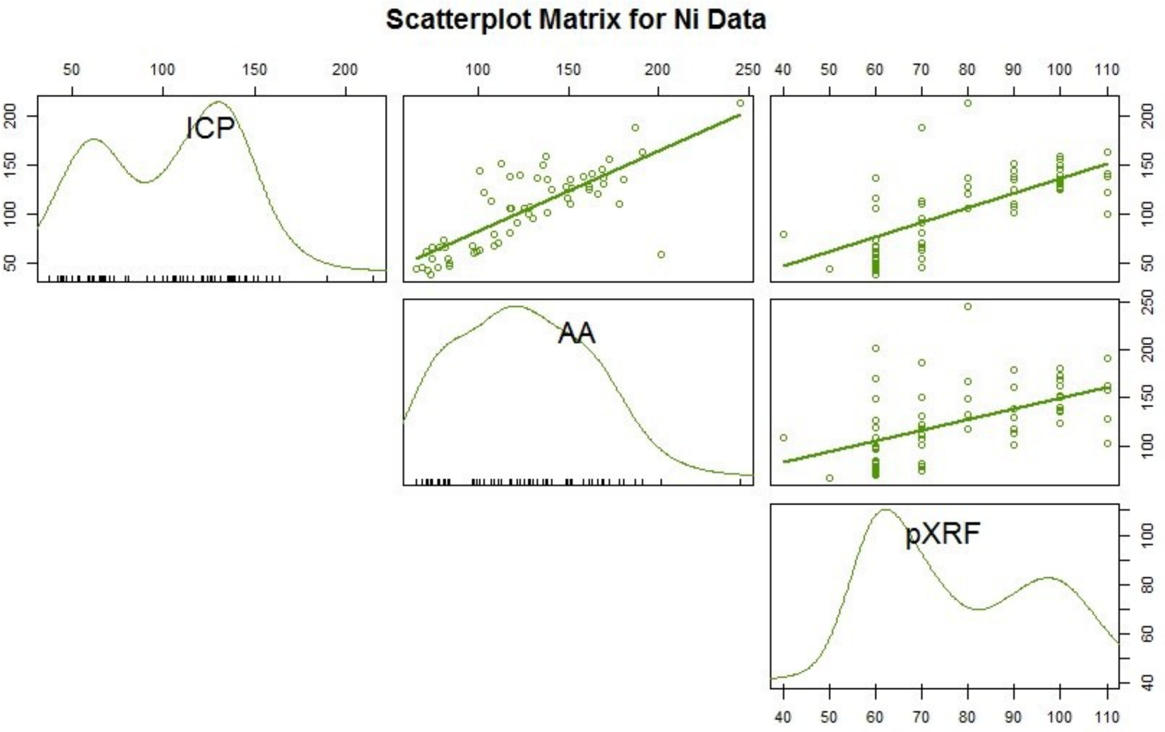

Figure 2.7 Scatterplot Matrix for Ni Data

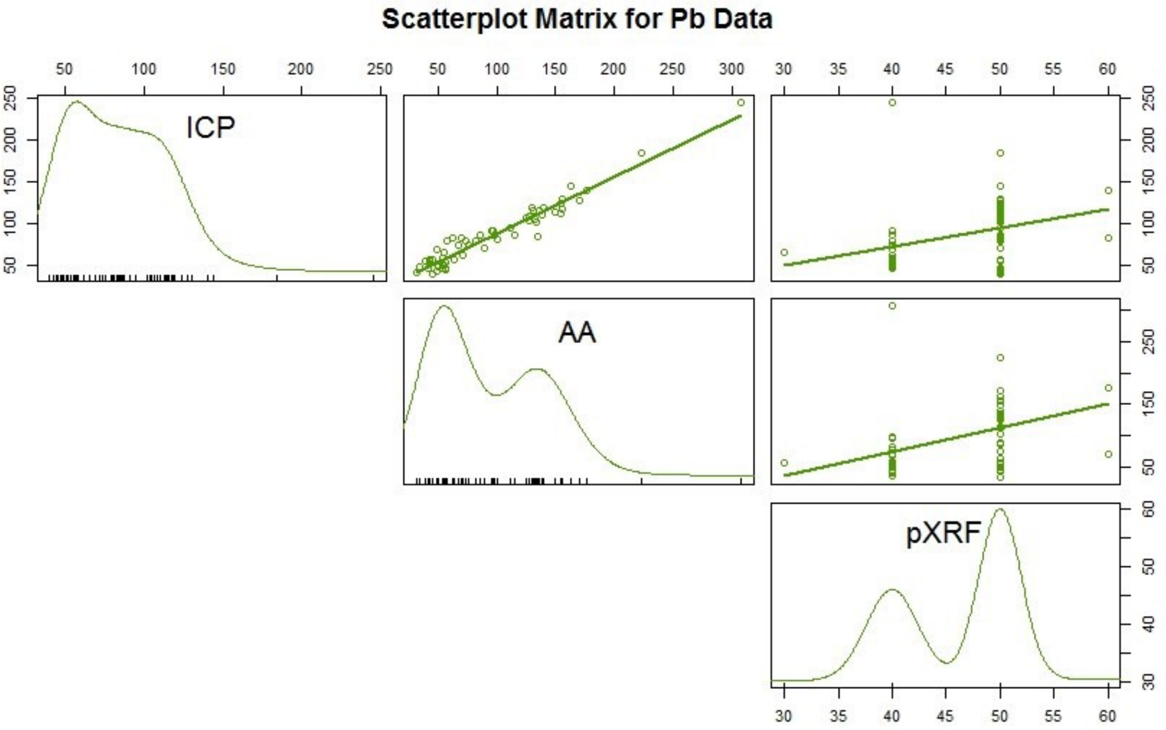

Figure 2.8 Scatterplot Matrix for Pb Data

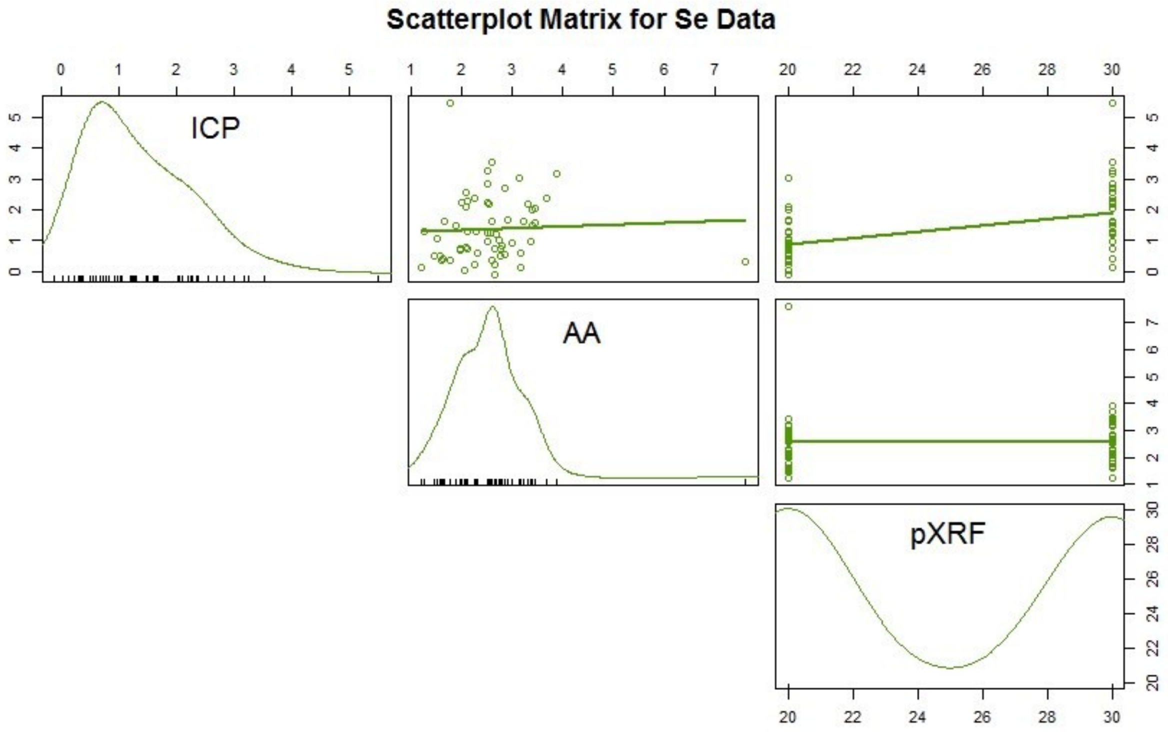

Figure 2.9 Scatterplot Matrix for Se Data

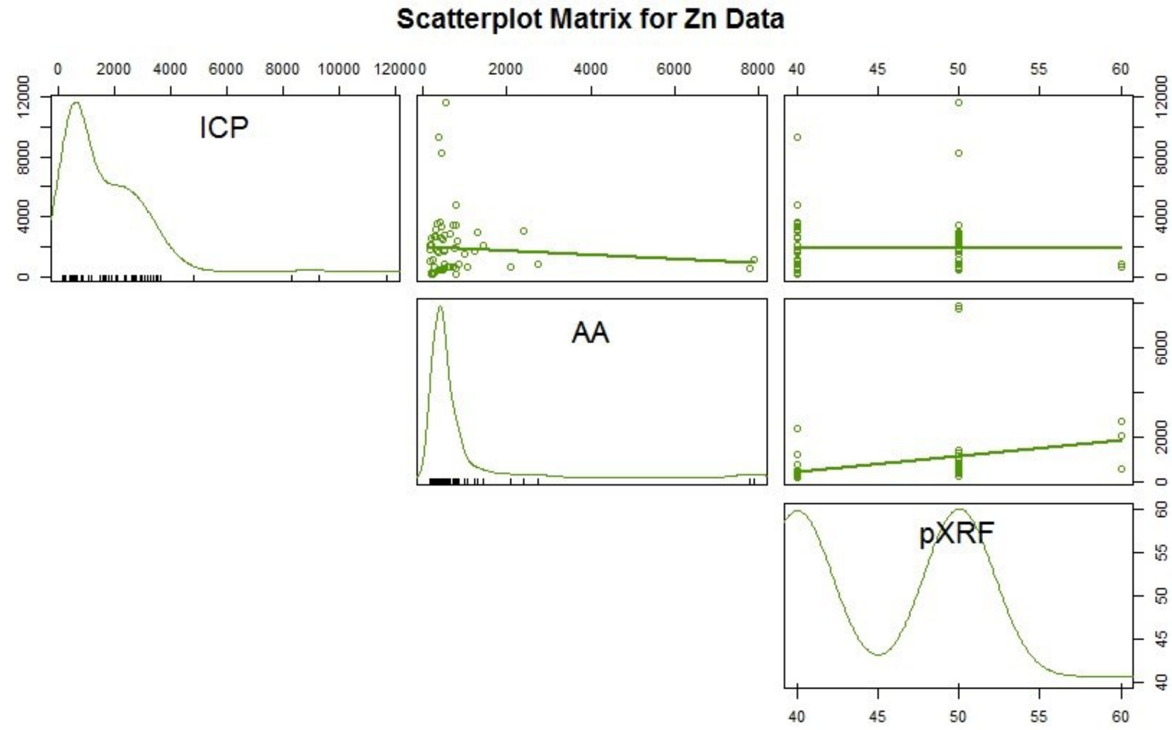

Figure 2.10 Scatterplot Matrix for Zn Data

CHAPTER III

EXPLORING PREDICTORS OF HEAVY METAL QUANTITIES THROUGH OBSERVED RELATIONSHIPS BETWEEN SOIL TYPE, LAND USE, DISTANCE TO ROADS, AND pH

Abstract

Environmental contamination is a topic that readily can be overlooked due to lax environmental regulations regarding remediation. This is especially true and more likely to occur in impoverished areas. The Rio Grande Valley is susceptible to such contamination due to its agricultural irrigation from the Rio Grande River, which contamination has been detected in from time to time. Following data from a 2002 study from UT El-Paso which detected the presence of As, Cr, Cu, Ni, Pb, and Zn in the water column of the Rio Grande in their region, this research was conducted to test for contamination in Rio Grande Valley agricultural soils. A total of 59 agricultural soil samples taken at 7 different locational sites were analyzed for heavy metals by Inductively Coupled Plasma Mass Spectrometry (ICP-MS). We examined and searched for heavy metal relationships by intended land use, distance from nearest road, soil type, and soil pH in order to predict patterns of heavy metal pooling due to increasing urbanization in the region. Statistical methods used for analysis include Kruskal-Wallis Rank Sum Tests and Redundancy Analyses (multivariate analysis similar to regression techniques) which were run in R Studio and Canoco 5 software respectively. Results show significant differences in both Cd and Fe based on soil type. The same is true for Cu in intended land use and distance from roads. There were no significant trends or correlations based on pH.

Introduction

As urbanization continues to proliferate across the world, concerns of heavy metal contamination as a result of urbanized environments in agricultural soils must be addressed to protect the health of the communities who live along these rural-urban gradients (McClintock, 2012). Urban soils are often contaminated with Cd, Cu, Pb, Zn, and these heavy metals are linked to traffic and other anthropogenic sources (Alloway, 2013; Gan et.al, 2018). Though naturally present in some amount in most soils, accumulation of anthropogenic pollution through windblown dust and debris from vehicles, buildings, and impervious services, along with storm water runoff may increase urban resident exposure to these chemical elements, all of which can have deleterious, toxic effects, especially when hyper-accumulated in produce grown in such soils.

With the advent of accurate accessible soil testing technology (Youwakim et al, chapter II) researchers have documented reliable predictors of heavy metal concentrations in soils to both help prevent and mitigate human exposure to toxic heavy metals. For example, Yan et al., (2012) found that proximity to road was an important predictor of Cd, Cu, Pb, and Zn in agricultural soils in Nepal, largely attributed to vehicle traffic along these roads. Soils proximate to concentrations of buildings and other aspects of urbanization are also associated with higher concentrations of these elements (Wang et al., 2018). In many cases, heavy metals can be predicted by soil characteristics, depending on the metals and their relationship respective to pH, soil type, and other soil physical/chemical properties (Zhang, et al., 2018; Kurame, 2012).

This research examines the reliability of those predictors in the rich alluvial soils of the lower Rio Grande Valley in Deep South Texas along the U.S.-Mexico Border. Urban populations along this region are projected to reach approximately 1.5 million by 2050 (Texas Demographic Center, 2019). Even now, has become increasingly urbanized, resulting in drastic rural-to-urban gradients, with a mosaic of agricultural use areas (farms) and unincorporated residential communities at the fringe. The region is home to more than 900 colonias, unincorporated neighborhoods that are usually lacking in one or more municipal services such as electricity, drinking water, sewage, or paved roads (Barton et. al., 2015). Food security is an issue in these communities (Barton et. al., 2015), and many initiatives to promote food access and community gardening are often well received. However, these communities are also embedded in areas that are highly at risk for soil contamination (Ramirez-Andreotta, 2014) due to poor drainage, irrigation runoff contaminated by sewage, and the use of pesticides or fertilizers, and concentrations of heavy metal contaminants associated with urbanized environments (da Silva, 2016).

In this work, we characterize heavy metal concentrations in various soils collected along this urban-rural gradient and explore various factors that could serve as predictors to heavy metal exposure in soils. We examine whether proximity to roads subject fields and farms to higher heavy metal concentrations, and explore the relationship of these concentrations to soil type and other soil conditions, such as pH. We present these findings within a broader discussion of soils management in this region, especially in the context of farms and other food production land uses such as community gardens in Colonias and other residential communities.

Materials and Methods

Site Description and Sample Collection

A total of 59 agricultural soil samples at 7 different locations were gathered non-randomly across both Starr and Hidalgo County in Deep South Texas. Samples include a mix of soils from citrus groves, grain fields, urban farms, and community gardens in various colonias. Sample locations were chosen based on permission granted from various farmers and landowners. Coordinates for each sampling site were recorded using a handheld GPS (Juno® SA, Trimble Sunnyvale, CA), and are listed in Table 3.2. Each of the 59 samples were composed of 6 soil cores taken using step-down soil corers (AMS) at depths of no greater than 30cm and between 1m- 130 m apart. Samples were taken compositely and mixed with the intention of testing for relationships between metal content and distance from roads. Soils were collected and stored at room temperature until processing. Samples described by soil type, soil pH, and distance to a main paved road (for three locations under farm in Table 3.2). Soil types were determined by in lab soil texture analyses using Soil Survey Field and Laboratory Methods Manual (NRCS, 2009) and soil pH was measured by a slurry (mixed with pH stirrer) of soil and deionized water (1:2 ratio) with a pH meter (B30PCI, sympHony) following methods from the Agriculture Laboratory Proficiency (ALP) Program (CTS, 2007). Distance to road was estimated referencing the GPS coordinates on a map and the distance measuring tool on Google Earth.

Sample Preparation and Digestion

The method used for digestion of soils is an adapted version of EPA 3050B used by the Texas Plant and Soil Lab and detailed in Test Methods for the Examination of Compost and Composting (U.S. Composting Council, 2002), where local participants would be most likely to send their samples for analysis. Samples were numbered and stored in laboratory conditions until processing and digestion. Samples were dried for 12 hours at 91°C in a precision oven (Lindberg blue). Samples were ground by hand in mortar and pestles and then sieved to 2mm.

1-gram samples of sieved soil were then weighed out in 2.5 x 20cm test tubes. 10mL of 35% nitric acid (HNO_3) were added to each sample in a test tube digestion block (SPB 50-24 PerkinElmer). Samples were then refluxed for 15 minutes at 95°C. Another 5 mL of 35% nitric acid (HNO_3) were then added and the samples were refluxed for another 30 minutes. Then, 3mL of 37% hydrochloric acid (HCl) were added and samples were heated at one hour in the test tube block, still at 95°C. After this step, the digestion block temperature was lowered to 80°C. 3 mL of 30% hydrogen peroxide (H_2O_2) were added with a 5 minute resting period before adding an additional 1mL with 5 min intervals until no more than 10mL of hydrogen peroxide (H_2O_2) were added (in order to avoid bubbling over and losing sample). If a drop was added and there was no reaction, the participant could stop adding hydrogen peroxide, however, this did not occur with any of our samples. The digestion block temperature was then raised again to 95°C before adding 10mL of deionized water. Samples were then refluxed for 15 min at 95°C. The digestion block was then turned off and samples were diluted with deionized water in 100mL volumetric flasks. Samples were stored at room temperature until further processing to be read on an Inductively Coupled Plasma Mass Spectrometer (ICP-MS, Agilent 7500ce) at the ICP-MS Lab in the Jackson School of Geosciences at the University of Texas at Austin (Miller, 2019). Samples were initially diluted by 25 in order to protect the ICP-MS
from any potential unknown quantities of high levels of contamination. Samples were read for As, Cd, Cr, Cu. Fe, Ni. Pb, Se, and Zn in a 2% (HNO_3) matrix.

Data Analysis

Results by site for 9 of the most common heavy metals are depicted in Table 3.2. Data were organized by location, land use, and distance from road (see Table 3.1). A constrained redundancy analysis (RDA) was run using Canoco 5 ™ (Lepš et al., 2003) to explore the relationships between heavy metal content of each of the 9 heavy metals and the following factors: soil type, distance to road, and pH. A second RDA was run to explore associations between heavy metals and soil particle size (clay, silt, and sand). Based on these analyses, we tested the statistical relationships of both soil type and distance to roads as predictors for the ICP-MS data for each of the aforementioned 9 heavy metals. Cumulative data from the ICP-MS analysis were non-parametric and unable to be normalized (Gan, et. al, 2018). Kruskal-Wallis Rank Sum Tests were used to explore the significance of soil type on ICP-MS data. Mann Whitney U tests were used for pairwise comparisons between metal and soil type. The Holm p-value adjustment method was utilized. To explore the associations between heavy metal and proximity to road we limited our analysis to the three locations where samples were collected along a gradient of distance to road. Shapiro-Wilks test for normality were run for each of the nine metals for each of these locations in order to determine the correct correlation method. Of the metals that showed negative correlations, all distributions were normal. Pearson's and Spearman's correlation coefficients were calculated and tested for significance. All statistical analyses were run in RStudio™ (Rstudio, 2020, Boston, MA).

Results

Land Use

No differences were found in average concentration of heavy metals between agriculture sites (n=31) and soil in residential locations (colonias and urban farms) (n=26), except for Cu, (H=10.99, 1 d.f., *P*=0.0009115), where soil from residential areas (162.25 ± 69.42 ppb) had more than 60% more Cu than in agricultural soils (106.56 ± 49.94 ppb). Mann Whitney U test results for Cu, (W = 196, p-value = 0.0007042), were used to compare the distribution of the Cu content between residential land and land intended for agricultural use. All other metals did not prove statistically significant using the Kruskal-Wallis Rank Sum Test. The following figure illustrates samples collected with their respective means denoted by the magenta crossed circle.

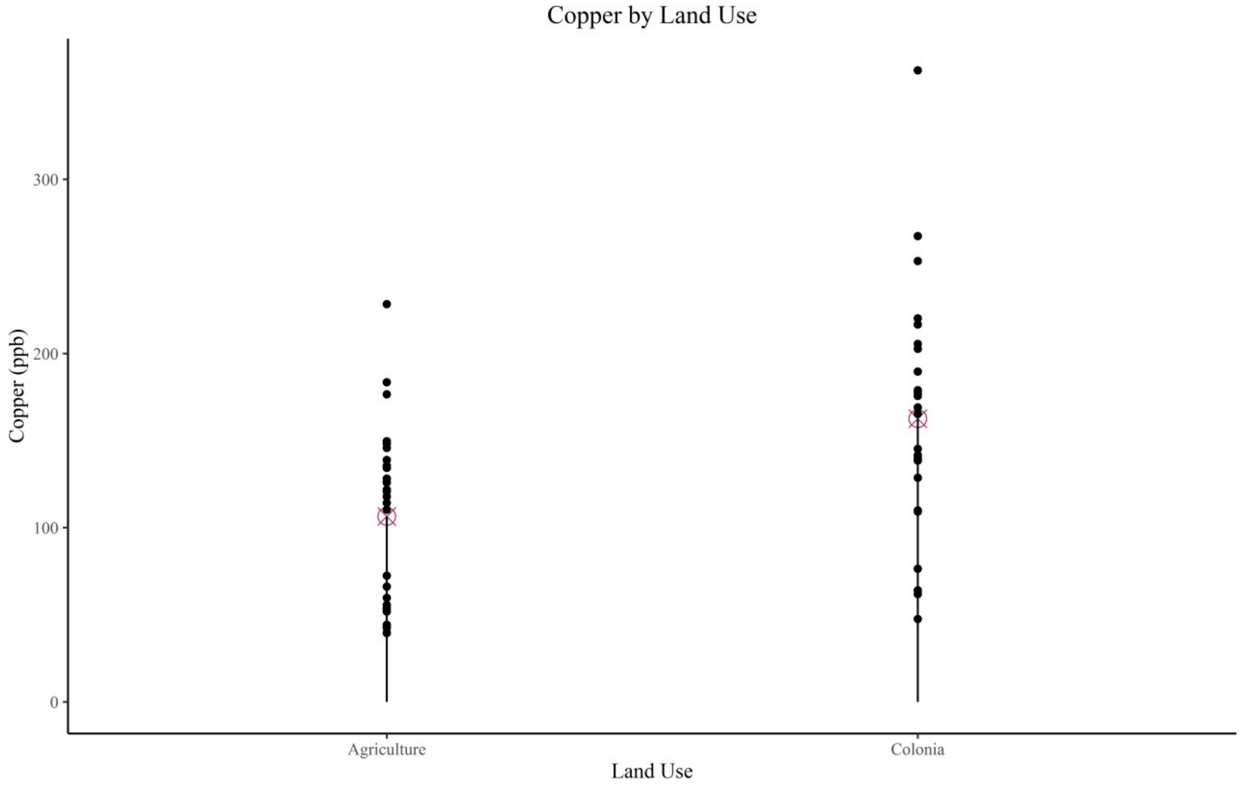

Figure 3.1 Copper by Land Use in ppb

Distance to main road

Data points for testing if metal content is correlated with distance from nearest road were tested by three locations: a citrus grove in Edinburg, TX (sites 2; composite samples n=4), a cattle pasture and three grain farms in Mercedes, TX (sites 4; composite samples n=14), and two grain farms in San Isidro, TX (sites 2; composite samples n=8). Below are the Pearson's and Spearman's correlation coefficients and p-values for all metals. The five metals that demonstrated a trend of higher metal content closer to roads are Cu in Edinburg, Cd, Cu, and Pb in Mercedes, and Zn in San Isidro. All significant trends are presented in bold font.

Table 3.1 Pearson Data for Metal Averages by Location

Location	As	Cd	Cr	Cu	Fe	Ni	Pb	Se	Zn
Edinburg	r = 0.2, r_s = 0.61	r = 0.40, r_s = 0.99	r = 0.49, p = 0.51	r = -0.26, p = 0.74	r = 0.87, p = 0.13	r = 0.23, p = 0.77	r = 0.68, p = 0.32	**r = 0.963, p = 0.037**	**r = 0.998, p = 0.002**
Mercedes	r = 0.62, p = 0.06	r = -0.084, p = 0.82	r = 0.34, p = 0.34	**r = -0.687, p = 0.028**	r = 0.26, p = 0.46	r = 0.59, p = 0.08	r = -0.37, p = 0.29	r = 0.18, p = 0.62	r = 0.62, r_s= 0.097
San Isidro	r = 0.48, p = 0.23	r = 0.39, p = 0.34	**r = 0.83, p = 0.01**	**r = 0.76, p = 0.03**	**r = 0.865, p = 0.0055**	r = 0.61, p = 0.11	r = 0.37, p = 0.37	r = 0.09, p = 0.83	r= -0.277, p = 0.51

All other metals actually showed an almost neutral relationship and some even showed very positive relationships, leaving us with very little evidence that in the samples collected distance from roads is a predictor of heavy metal content in soil. However, the sample size for all locations is under 30 samples, so we hope that this may provide incentive for more sampling.

pH

Statistics analyzing pH were run using scatterplots with Spearman's correlations, but no significant correlations were found. Soil pH range for collected samples was 7.36-8.23.

Soil Type

Soil type was a weak predictor for most heavy metal concentrations, except for Cd (H=7.023, 2 d.f., *P*=0.0298) and Fe (H=6.54, 2 d.f., *P*=0.0381). The below table illustrates mean ± standard deviation, followed by letters that identify the significance of the pairwise comparisons.

Table 3.2 Soil Type Summary Statistics and Pairwise Comparisons in ppb

	Cd	**Fe**
Sandy Clay Loam (SCL)	3.97 ± 0.65 A	162761.44 ± 15078.39 A
Sandy Loam (SL)	3.14 ± 1.03 AB	98065.46 ± 48112.62 B
Loamy Sand (LS)	2.75 ±1.01 B	79506.06 ± 31498.89 B

All other metals did not prove statistically significant using the Kruskal-Wallis Rank Sum Test nor were there any significant pairwise comparisons. The data are provided below.

Table 3.3 Non-Significant Soil Type Summary Statistics and Pairwise Comparisons in ppb

	As	**Cr**	**Cu**	**Ni**	**Pb**	**Se**	**Zn**
SCL	14.16 ± 3.37	148.80 ± 5.27	148.91 ± 15.08	139.04 ± 17.54	111.75 ± 10.28	2.08 ± 0.43	1950.77 ± 872.77
SL	14.83 ± 11.94	98.55 ± 38.51	130.15 ± 62.58	99.09 ± 40.05	89.16 ± 43.31	1.45 ± 1.21	1804.75 ± 2090.85
LS	17.45 ± 8.76	92.91 ± 48.04	138.33± 79.87	100.79 ± 44.38	71.82 ± 20.66	0.99 ± 0.68	2416.59 ± 2505.34

Modeling Predictors

A constrained redundancy analysis (RDA) was run in Canoco 5 software due to the linear distribution of the ICP data and in order to visually represent an ordination analysis overlaying our quantitative and qualitative data. Soil types are abbreviated SL for Sandy Loam, LS for

Loamy Sand, and SCL for Sandy Clay Loam. This RDA illustrates likelihood for higher metal content to be found in SCL, with little relationship found between SL or LS. Results show trends for As and Zn to follow the hypothesis of higher metal content being more likely to be detected closer to a road, with all other metals trending in the opposite direction. There is a slightly greater likelihood of metal content being higher in Colonias over Agricultural lands, with a focus on Zn in particular. As discussed in prior correlation analysis, there is no relationship to pH. Permutation test results prove significance with a p-value of 0.002.

Figure 3.2 RDA Predictor Model for Soil Characteristics

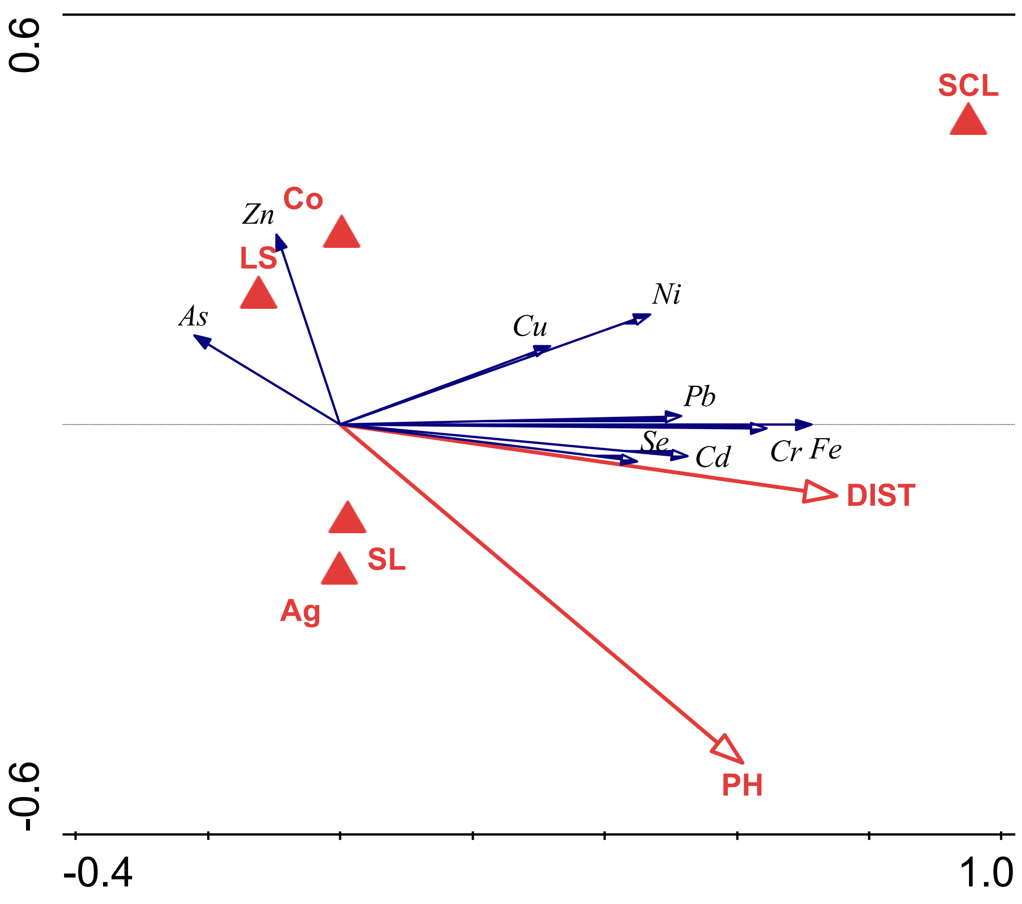

Total variation is 99146927378.298, explanatory variables account for 50.7% (Adjusted explained variation is 45.1%).

Table 3.4 Summary Table for Soil Characteristics

<table>
<tr><th colspan="2">Statistic</th><th colspan="2">Axis 1</th><th>Axis 2</th></tr>
<tr><td colspan="2">Eigenvalues</td><td colspan="2">0.5068</td><td>0.0002</td></tr>
<tr><td colspan="2">Explained variation (cumulative)</td><td colspan="2">50.68</td><td>50.70</td></tr>
<tr><td colspan="2">Pseudo-canonical correlation</td><td colspan="2">0.7129</td><td>0.2851</td></tr>
<tr><td colspan="2">Explained fitted variation (cumulative)</td><td colspan="2">99.96</td><td>100.00</td></tr>
<tr><td colspan="5">Per-Axis Statistics</td></tr>
<tr><td>Statistic</td><td>Axis 1</td><td>Axis 2</td><td>Axis 3</td><td>Axis 4</td></tr>
<tr><td>Origin Scores</td><td>-2.86354</td><td>-4.14503</td><td>0.00000</td><td>0.00000</td></tr>
<tr><td>Extracted from expl. data</td><td>0.17893</td><td>0.22595</td><td>0.00000</td><td>0.00000</td></tr>
<tr><td colspan="5">Permutation Test Results</td></tr>
<tr><td colspan="2">Statistic</td><td colspan="3">Value</td></tr>
<tr><td colspan="2">Pseudo-F</td><td colspan="3">9.1, d.f. 5</td></tr>
<tr><td colspan="2">p-value</td><td colspan="3">0.00200</td></tr>
<tr><td colspan="2">Number of permutations</td><td colspan="3">499</td></tr>
</table>

Another constrained redundancy analysis (RDA) was run in Canoco 5 software in order to observe more closely the effects of soil composition on metal content. This RDA show clay content as a strong predictor for Cu, Pb, Se, Cd, Cr, Ni, and Fe. Permutation test results prove significance with a pseudo-F of 6.9, d.f. 2, and p-value of 0.004, and 499 permutations.

Figure 3.3 RDA Predictor Model for Soil Composition

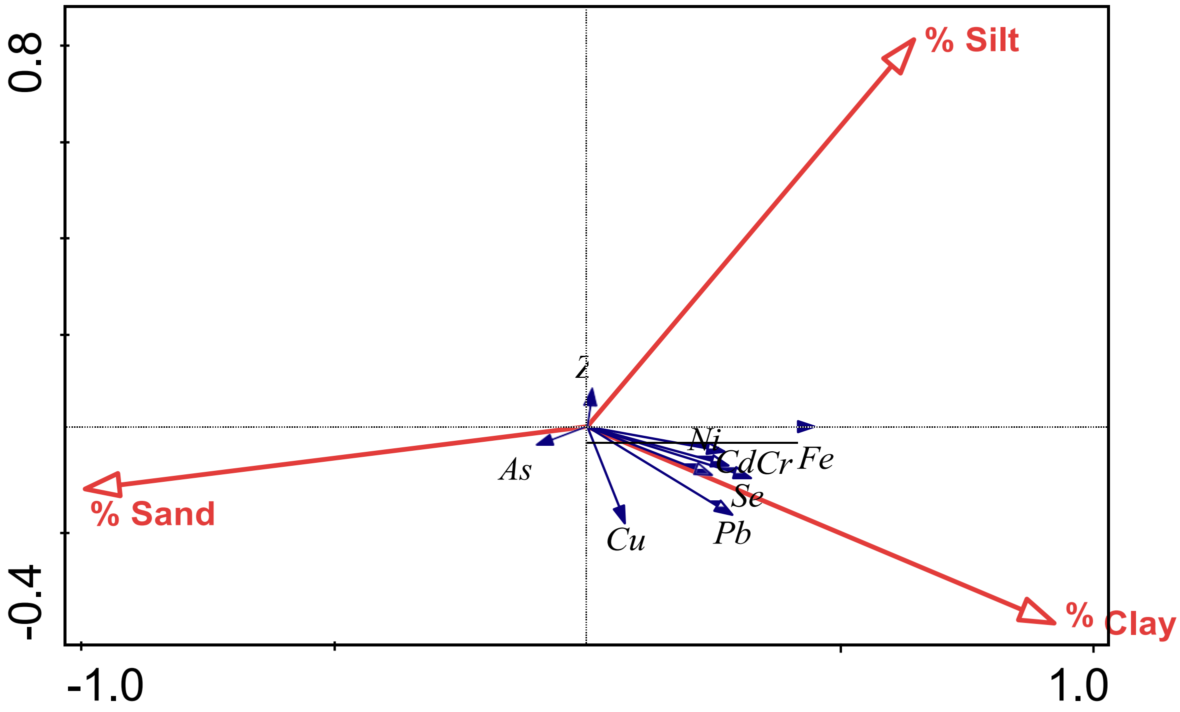

Total variation is 115882030658.903, explanatory variables account for 20.1%

(Adjusted explained variation is 17.2%).

Table 3.5 Summary Table for Soil Composition

Statistic	**Axis 1**	**Axis 2**	**Axis 3**	**Axis 4**
Eigenvalues	0.2007	0.0000	0.7970	0.0023
Explained variation (cumulative)	20.07	20.07	99.77	100.00
Pseudo-canonical correlation	0.4485	0.0767	0.0000	0.0000
Explained fitted variation (cumulative)	99.99	100.00	0.0000	0.0000
Per-Axis Statistics				
Statistic	**Axis 1**	**Axis 2**	**Axis 3**	**Axis 4**
Origin Scores	-4.77001	-11.49687	-2.39354	-0.98486
Extracted from expl. data	0.75010	0.24990	0.00000	0.00000

Discussion

Roadside contamination from heavy metals breaks down to cadmium emissions from lubrication oil consumption and tire wear, zinc emissions from fuel tanks and tire wear, copper and lead emissions from brake wear, and lead from worn metal alloys in the engine and exhaust gas from vehicles (Yan, 2012). Contrary to previous studies linking increasing distance from road to decreasing heavy metal concentrations (Yan, 2012), this study found that proximity to road is a poor predictor of heavy metal content in this region. This may mean that this region's traffic emissions are currently not great enough to affect heavy metal content or that countries where this is a consistent issue have less regulation enforcement over vehicle emissions. It could also mean that in countries suffering from heavy metal contamination where rapid urbanization and agricultural regions are proximally present have stricter governmental levels of heavy metal content that is considered contamination (Jia et. al., 2018). If possible, sampling on farms closer to busy roads may provide different results, however, it is not always simple to obtain sampling access to these areas.

Median household income for Colonias is almost half that of Texas who live outside of Colonias, and Colonia residents utilize public assistance programs more than their municipality residing neighbors (Barton et. al., 2015). While it is already an issue that communities of color are more likely to experience environmental pollution, these Texas border communities are at particular risk due to the majority Hispanic population which compromises 71-99% of border counties (Masten, et. al., 2016) (Texas Demographic Center, 2019). Per land use, we did not observe any results which would lead us to conclude inherent discrepancies between residential communities and agricultural land. This is a positive finding for the cause of the promotion of urban and community gardens to address issues of food access, food security and community prosperity. Our research may suggest that these kinds of initiatives would not expose residents interested in community gardening to heavy metals, at least in the areas we explored, which is not always the case for community gardens emerging in urban areas (Sharma, 2014).

For the Rio Grande Valley, it appears that sandy clay loam can be predictive of higher heavy metal concentrations relative to other soil types. It also comprised the smallest number of our soil samples, and as such there may be added benefit in conducting soil texture tests prior to digestion in order to ensure balanced sampling quantities for specific regions, if one is interested in mainly studying soil texture as a predictor for metal content. Speaking more generally for soils across the world, clay percentage may be the best predictor. As the Kruskal Wallis analysis only portrays this for Cd and Fe, this can signify a variety of conclusions. Cd in agricultural fields is sourced in part from phosphate-based fertilizers (da Silva, 2016), which may have been used in the fields we sampled in. Fe is not considered a toxic heavy metal, and is naturally present in soils, but can be toxic in higher quantities and is more harmful to plants than humans (Zwolak et. al., 2019). As for clay, soils with higher percentages of clay and soil organic matter (SOM) are more likely to have higher heavy metal concentrations than other soil types (Dube, 2001). This can be attributed to van der Waals forces, linkage of particles through cationic bridges, i.e. Fe^{+3}, Cd^{+2}, and the cementation effects of SOM (Chessworth et. al., 2008).

While there was no relationship found between pH and metal content, this may be due to the fact that the average pH of our soils was 7.84, and metal release is dependent on soil pH and varies greatly between metals (Zhang et. al, 2018). Lower pH levels are known to affect the bioavailability of Cd, Cu, Pb, and Zn (Chessworth et. al., 2008). In one study this was observed with Cd, showing a direct relationship between increasing Cd content of carbonate fractions and increasing pH between the 4.5-9.5 range (Zhang et. al, 2018).

The following table provides remediation levels for heavy metals in soils for the Texas Commission on Environmental Quality (TCEQ) and the Environmental Protection Agency (EPA). All samples in this study fell under both thresholds. We encourage the reader to note the discrepancy between the orders of magnitude depending on state or federal regulations.

Table 3.6 State and Federal Levels for Heavy Metal Contamination in Soil

Element of Concern	TCEQ Levels for Soil Remediation in .5 acre> in µg/l (ppb)	EPA Regulatory limits on Heavy Metals Applied to Soils in µg/l (ppb)
As-Arsenic	2.00E+03	7.50E+02
Cd-Cadmium	8.10E+03	8.50E+02
Cr-Chromium	1.20E+06	3.00E+04
Cu-Copper	9.40E+05	4.30E+04
Fe-Iron	N/A	N/A
Ni-Nickel	8.80E+04	7.50E+02
Pb-Lead	1.60E+04	4.20E+03
Se-Selenium	4.90E+04	8.40E+03
Zn-Zinc	2.50E+06	7.50E+04

(EPA, 2016; TCEQ, 2019)

It is excellent news to be able to report to farmers and Colonia residents that their soils were free of contamination, however, I would urge them to be vigilant as their communities experience economic expansion and urban development, as sources of soil contamination are likely to increase (Sharma, 2014).

CHAPTER IV

CONCLUSION

In this thesis we confirmed that the pXRF is a tool that cannot provide the accuracy of in lab techniques, but can provide a binary estimate response of contamination levels. We found trends in metals for different instruments, but our results show that the ICP-MS data still remains the most reliable. In our comparisons for distance and soil type, with more samples we could have provided stronger results. All in all, data is provided for researchers deciding which techniques may be most appropriate for their subjects of concern.

The following table provides average values of 47 samples for the elements of interest sampled throughout the Rio Grande from 2015-2018 by the International Boundary and Water Commission. We compare them to the average values obtained from our 59 samples in 2019 for the same elements. While they are higher for each element, when compared to the regulatory values from both the Texas Commission on Environmental Quality (TCEQ) and the Environmental Protection Agency (EPA), we did not detect contamination in any of our soil samples.

Table 4.1 “Dissolved in Water” Approximate Sampling Averages in the Rio Grande from 2015-2018 in µg/l (ppb)

	Element								
	As	Cd	Cr	Cu	Fe	Ni	Pb	Se	Zn
IBWC	10.12	1.8	8.84	11.17	68.02	3.71	13.64	6.43	25.44
RGV Soil	15.26	3.13	100.76	134.66	95453.43	103.97	87.02	1.39	1940.48

(U.S. International Boundary and Water Commission, Rio Grande Basin Texas Clean Rivers Program, 2020).

In retrospect, there exist tools for soil sampling which can provide more precise and consistent soil sampling depths, therefore for future work I recommend researchers use such tools to obtain soil depths of only 5cm or less, as concentrations can vary at different depths (Usman et al., 2017). I stress the importance of using consistent testing metrics with the provision of enough time to perform laboratory analysis in a precise and careful manner. Lastly, while this thesis did not discover any contamination, the Rio Grande Valley remains a highly susceptible region to heavy metal contamination and regular testing should be conducted whenever possible. It is my hope that the work in this thesis makes this testing more accessible to citizens of the Rio Grande Valley and across the world.

REFERENCES

Adamiec, E., Jarosz-Krzemińska, E., & Wieszała, R. (2016). Heavy metals from non-exhaust vehicle emissions in urban and motorway road dusts. *Environmental monitoring and assessment*, *188*(6), 369. https://doi.org/10.1007/s10661-016-5377-1

Allende, A., & Monaghan, J. (2015). Irrigation Water Quality for Leafy Crops: A Perspective of Risks and Potential Solutions. *International journal of environmental research and public health*, *12*(7), 7457–7477. https://doi.org/10.3390/ijerph120707457

Alloway B.J. (2013) Sources of Heavy Metals and Metalloids in Soils. In: Alloway B. (eds) Heavy Metals in Soils. Environmental Pollution, vol 22. Springer, Dordrecht

Baker, D. E., Amacher, M. C., & Leach, R. M. (1979). *Sewage sludge as a source of cadmium in soil–plant–animal systems. Environmental Health Perspectives, 28, 45–49.* doi:10.1289/ehp.792845

Ballabio, C., Panagos, P., Lugato, E., Huang, J.-H., Orgiazzi, A., Jones, A., … Montanarella, L. (2018). *Copper distribution in European topsoils: An assessment based on LUCAS soil survey. Science of The Total Environment, 636, 282–298.* doi:10.1016/j.scitotenv.2018.04.268

Barton, Jordana., Perlmeter, Emily., Marquez, Raquel. (2015). Las Colonias in the 21 st Century: Progress along the Texas-Mexico Border. *Federal Reserve Bank of Dallas.* www.dallasfed.org/~/media/documents/cd/pubs/lascolonias/pdf

Bauer, M., Fulda, B., & Blodau, C. (2008). *Groundwater derived arsenic in high carbonate wetland soils: Sources, sinks, and mobility. Science of The Total Environment, 401(1-3), 109–120.* doi:10.1016/j.scitotenv.2008.03.030

Binstock, David A.; Gutknecht, William F.; and McWilliams, Andrea C. (2009) "Lead in Soil - An Examination of Paired XRF Analysis Performed in the Field and Laboratory ICP- AES Results," *International Journal of Soil, Sediment and Water*: Vol. 2 : Iss. 2 , Article 1.
Available at: https://scholarworks.umass.edu/intljssw/vol2/iss2/1

Bruker. (2018). *Heavy Metals & Nutrients in Soil (P/N 730.0202)* [Brochure]

Chesworth W. et al. (2008) Clay-Organic Interactions. In: Chesworth W. (eds) Encyclopedia of Soil Science. Encyclopedia of Earth Sciences Series. Springer, Dordrecht https://doi.org/10.1007/978-1-4020-3995-9

da Silva, F.B.V., do Nascimento, C.W.A., Araújo, P.R.M. *et al* (2016). Assessing heavy metal sources in sugarcane Brazilian soils: an approach using multivariate analysis. *Environ Monit Assess* **188,** 457). https://doi.org/10.1007/s10661-016-5409-x

Declercq, Y., Delbecque, N., Grave, J. D., Smedt, P. D., Finke, P., Mouazen, A. M., … Verdoodt, A. (2019). A Comprehensive Study of Three Different Portable XRF Scanners to Assess the Soil Geochemistry of An Extensive Sample Dataset. *Remote Sensing*, *11*(21), 2490. doi: 10.3390/rs11212490

Dube, A. , R. Zbytniewski T. Kowalkowski , E. Cukrowska , B. Buszewski. (2001). Adsorption and Migration of Heavy Metals in Soil. *Polish Journal of Environmental Studies 10(1,) 1-10.*

Environmental Health and Medicine Education. (2013, December 10). Retrieved March 20, 2019, from https://www.atsdr.cdc.gov/csem/csem.asp?csem=6&po=12

Environmental Protection Agency (EPA). DONNA RESERVOIR AND CANAL SYSTEM DONNA, TX. (2020). Retrieved July 16, 2020, from https://cumulis.epa.gov/supercpad/SiteProfiles/index.cfm?fuseaction=second.Cleanup

EPA, Environmental Protection Agency, “Guidance for Developing Ecological Soil Screening Levels.” Sept. 29, 2016. Accessed April 28, 2020. www.epa.gov/chemical-research/guidance-developing-ecological-soil-screening-levels.

Gan, Yandong, Yongjun Miao, Lihong Wang, Guiqiang Yang, Yuncong C. Li, Wenxing Wang, and Jiulan Dai. (2018). Source Contribution Analysis and Collaborative Assessment of Heavy Metals in Vegetable-Growing Soils. *Journal of Agricultural and Food Chemistry* **2018** *66* (42), 10943-1095. DOI: 10.1021/acs.jafc.8b04032

Ghazi, F. Farah. (2018). Estimation of Heavy Metals Contamination in the Soil of Zaafaraniya City Using the Neural Network. J. Phys.: Conf. Ser. 1003 012058

Gochfeld, M., & Burger, J. (2011). Disproportionate exposures in environmental justice and other populations: the importance of outliers. *American journal of public health*, *101 Suppl 1*(Suppl 1), S53–S63. https://doi.org/10.2105/AJPH.2011.300121

Hanesch, M., Scholger, R., & Dekkers, M. J. (2001). *The application of fuzzy C-means cluster analysis and non-linear mapping to a soil data set for the detection of polluted sites. Physics and Chemistry of the Earth, Part A: Solid Earth and Geodesy, 26(11-12), 885–891.* doi:10.1016/s1464-1895(01)00137-5

Heijerick, D. G., Van Sprang, P. A., & Van Hyfte, A. D. (2006). *AMBIENT COPPER CONCENTRATIONS IN AGRICULTURAL AND NATURAL EUROPEAN SOILS: AN OVERVIEW. Environmental Toxicology and Chemistry, 25(3), 858.* doi:10.1897/04-671r.1

Holmgren, G. G. S., Meyer, M. W., Chaney, R. L., & Daniels, R. B. (1993). *Cadmium, Lead, Zinc, Copper, and Nickel in Agricultural Soils of the United States of America. Journal of Environment Quality, 22(2), 335.* doi:10.2134/jeq1993.00472425002200020015x

Hu, W., Huang, B., Weindorf, D. C., & Chen, Y. (2014). *Metals Analysis of Agricultural Soils via Portable X-ray Fluorescence Spectrometry. Bulletin of Environmental Contamination and Toxicology, 92(4), 420–426.* Doi:10.1007/s00128-014-1236-3

Jaishankar, M., Tseten, T., Anbalagan, N., Mathew, B. B., & Beeregowda, K. N. (2014). Toxicity, mechanism and health effects of some heavy metals. *Interdisciplinary toxicology*, *7*(2), 60–72. https://doi.org/10.2478/intox-2014-0009

Jia, Z., Li, S. & Wang, L. Assessment of soil heavy metals for eco-environment and human health in a rapidly urbanization area of the upper Yangtze Basin. *Sci Rep* **8,** 3256 (2018). https://doi.org/10.1038/s41598-018-21569-6 Jing, F., Chen, X., Yang, Z. et al. Environ Earth Sci (2018) 77:104. https://doi.org/10.1007/s12665-018-7299-4,

J.S. Rieuwerts, I. Thornton, M.E. Farago & M.R. Ashmore (1998) Factors influencing metal bioavailability in soils: preliminary investigations for the development of a critical loads approach for metals, Chemical Speciation & Bioavailability, 10:2, 61-75, DOI: 10.3184/095422998782775835

Karar, K., Gupta, A. K., Kumar, A., & Biswas, A. K. (2006). *Characterization and Identification of the Sources of Chromium, Zinc, Lead, Cadmium, Nickel, Manganese and Iron in Pm10 Particulates at the Two Sites of Kolkata, India. Environmental Monitoring and Assessment, 120(1-3), 347–360.* doi:10.1007/s10661-005-9067-7

Kilbride, C., Poole, J., & Hutchings, T. R. (2006). A comparison of Cu, Pb, As, Cd, Zn, Fe, Ni and Mn determined by acid extraction/ICPeOES and ex situ field portable X-ray fluorescence analyses. *Environmental Pollution*, 16–23. doi: 10.1016/j.envpol.2005.11.013

Kim, S.-M., & Choi, Y. (2019). Mapping Heavy Metal Concentrations in Beach Sands Using GIS and Portable XRF Data. *Journal of Marine Science and Engineering*, *7*(2), 42. doi: 10.3390/jmse7020042

Kuramae, Eiko E. Etienne Yergeau, Lina C. Wong, Agata S. Pijl, Johannes A. van Veen, George A. Kowalchuk, Soil characteristics more strongly influence soil bacterial communities than land-use type, *FEMS Microbiology Ecology*, Volume 79, Issue 1, January 2012, Pages 12–24, https://doi.org/10.1111/j.1574-6941.2011.01192.x

Lagalante, A. F. (2004). *Atomic Absorption Spectroscopy: A Tutorial Review*. Applied Spectroscopy Reviews, 34(3), 173–189.* doi:10.1081/asr-

Lamine, S., Petropoulos, G., Brewer, P., Bachari, N.-E.-I., Srivastava, P., Manevski, K., … Macklin, M. (2019). Heavy Metal Soil Contamination Detection Using Combined Geochemistry and Field Spectroradiometry in the United Kingdom. *Sensors*, *19*(4), 762. doi:10.3390/s19040762

LARSEN, E., MOSEHOLM, L., & NIELSEN, M. (1992). *Atmospheric deposition of trace elements around point sources and human health risk assessment. II: Uptake of arsenic and chromium by vegetables grown near a wood preservation factory. Science of The Total Environment, 126(3), 263–275.* doi:10.1016/0048-9697(92)90201-3z

Lemière, B. (2018). *A review of pXRF (field portable X-ray fluorescence) applications for applied geochemistry. Journal of Geochemical Exploration, 188, 350–363.* doi:10.1016/j.gexplo.2018.02.006

Lepš, J., & Šmilauer, P. (2003). *Multivariate analysis of ecological data using CANOCO*. Cambridge, UK: Cambridge University Press.

Liang, J.; Li, W.; Bradford, S.A.; Šimůnek, J. Physics-Informed Data-Driven Models to Predict Surface Runoff Water Quantity and Quality in Agricultural Fields. *Water* **2019**, *11*, 200.

Marguí, E., Hidalgo, M., & Queralt, I. (2007). XRF Spectrometry for Trace Element Analysis of Vegetation Samples. *Spectroscopy Europe*, *19* (3), 13–17.

Masten, S. J., Davies, S. H., & Mcelmurry, S. P. (2016). Flint Water Crisis: What Happened and Why?. *Journal - American Water Works Association*, *108*(12), 22–34. https://doi.org/10.5942/jawwa.2016.108.0195

McClintock, Nathan. (2012). Assessing Soil Lead Contamination at Multiple Scales in Oakland, California: Implications for Urban Agriculture and Environmental Justice. *Applied Geography 35(1-2):*460-473. Doi: 10.1016/j.apgeog.2012.10.001

McComb, J. Q., Rogers, C., Han, F. X., & Tchounwou, P. B. (2014). Rapid screening of heavy metals and trace elements in environmental samples using portable X-ray fluorescence spectrometer, A comparative study. *Water, air, and soil pollution*, *225*(12), 2169. https://doi.org/10.1007/s11270-014-2169-5

Mendoza, J., Botsford, J., Hernandez, J., Montoya, A., Saenz, R., Valles, A., Vazquez, A., & Alvarez, M. (2004). Microbial contamination and chemical toxicity of the Rio Grande. *BMC microbiology*, *4*, 17. https://doi.org/10.1186/1471-2180-4-17

Nriagu, J. O., Bhattacharya, P., Mukherjee, A. B., Bundschuh, J., Zevenhoven, R., & Loeppert, R. H. (2007). *Arsenic in soil and groundwater: an overview. Arsenic in Soil and Groundwater Environment - Biogeochemical Interactions, Health Effects and Remediation, 3–60.* doi:10.1016/s1875-1121(06)09001-8

Peña-Icart, M., Villanueva Tagle, M. E., Alonso-Hernández, C., Rodríguez Hernández, J., Behar, M., & Pomares Alfonso, M. S. (2011). Comparative study of digestion methods EPA 3050B (HNO_3--H_2O_2--HCl) and ISO 11466.3 (aqua regia) for Cu, Ni and Pb contamination assessment in marine sediments. *Marine environmental research*, *72*(1-2), 60–66. https://doi.org/10.1016/j.marenvres.2011.05.005

PerkinElmer. (2018). *World Leader in AA, ICP-OES and ICP-MS: Atomic Spectroscopy - A Guide to Selecting the Appropriate Technique and System.* [Brochure]. Author. Retrieved July 7, 2020, from https://www.perkinelmer.com/lab-solutions/resources/docs/BRO_WorldLeaderAAICPMSICPMS.pdf

Pyle, S. M., Nocerino, J. M., Deming, S. N., Palasota, J. A., Palasota, J. M., Miller, E. L., … Nichols, K. D. (1996). Comparison of AAS, ICP-AES, PSA, and XRF in Determining Lead and Cadmium in Soil. *Environmental Science & Technology*, *30*(1), 204–213. doi: 10.1021/es9502482

Radu T, Diamond D. Comparison of soil pollution concentrations determined using AAS and portable XRF techniques. *J Hazard Mater*. 2009;171(1-3):1168-1171. doi:10.1016/j.jhazmat.2009.06.062

Ramirez-Andreotta MD, Brody JG, Lothrop N, Loh M, Beamer PI, Brown P. Improving Environmental Health Literacy and Justice through Environmental Exposure Results Communication. *Int J Environ Res Public Health*. 2016;13(7):690. Published 2016 Jul 8. doi:10.3390/ijerph13070690

Ramirez-Andreotta, M. D., Brusseau, M. L., Artiola, J. F., & Maier, R. M. (2013). A greenhouse and field-based study to determine the accumulation of arsenic in common homegrown vegetables grown in mining-affected soils. *The Science of the total environment*, *443*, 299–306. https://doi.org/10.1016/j.scitotenv.2012.10.095

Ramirez-Andreotta, M. D., Lothrop, N., Wilkinson, S. T., Root, R. A., Artiola, J. F., Klimecki, W., & Loh, M. (2016). Analyzing Patterns of Community Interest at a Legacy Mining Waste Site to Assess and Inform Environmental Health Literacy Efforts. *Journal of environmental studies and sciences*, *6*(3), 543–555. https://doi.org/10.1007/s13412-015-0297-x

Ridings, M., Shorter, A.J. and Bawden-Smith, J. (2000) Strategies for the investigation of Contaminated Sites using Field Portable X-Ray Fluorescence (FPXRF) Techniques. Communications in Soil Science and Plant Analysis 31, 11-14, 1785-1790

Rios-Arana, J., Walsh, E., & Gardea-Torresdey, J. (2003). Assessment of arsenic and heavy metal concentrations in water and sediments of the Rio Grande at El Paso–Juarez metroplex region. *Environment International, 29*(7), 957-971. doi:10.1016/s0160-4120(03)00080-1

RStudio Team (2020). RStudio: Integrated Development for R. RStudio, PBC, Boston, MA URL http://www.rstudio.com/.

Selim, H. M. E. (2017). *Competitive sorption and transport of heavy metals in soils and geological media*. Boca Raton: CRC Press, Taylor & Francis Group.

Selim, H. M. E., & Iskandar, I. K. (1999). *Fate and transport of heavy metals in the vadose zone*. Boca Raton, FL: Lewis Publishers.

Sharma, K., Basta, N. T., & Grewal, P. S. (2014). *Soil heavy metal contamination in residential neighborhoods in post-industrial cities and its potential human exposure risk. Urban Ecosystems, 18(1), 115–132.*

Siddiqui, S., Conkle, J. L., Scarpa, J., & Sadovski, A. (2020). *An analysis of U.S. wastewater treatment plant effluent dilution ratio: Implications for water quality and aquaculture. Science of The Total Environment, 721, 137819.* doi:10.1016/j.scitotenv.2020.137819

Sparks, D. L., Soil Science Society of America., & American Society of Agronomy. (1996). *Methods of soil analysis: Part 3*. Madison, Wis: Soil Science Society of America.

Srivastava Vaibhav, Sarkar Abhijit, Singh Sonu, Singh Pooja, de Araujo Ademir S. F., Singh Rajeev P. (2017). Agroecological Responses of Heavy Metal Pollution with Special Emphasis on Soil Health and Plant Performances. *Frontiers in Environmental Science(5)* 64. DOI:10.3389/fenvs.2017.00064

Suman, J., Uhlik, O., Viktorova, J., & Macek, T. (2018). Phytoextraction of Heavy Metals: A Promising Tool for Clean-Up of Polluted Environment?. *Frontiers in plant science*, *9*, 1476. https://doi.org/10.3389/fpls.2018.01476

Sun, G. L., Reynolds, E. E., & Belcher, A. M. (2019). Designing yeast as plant-like hyperaccumulators for heavy metals. *Nature communications*, *10*(1), 5080. https://doi.org/10.1038/s41467-019-13093-6

TCEQ. (2018, April 27). 23rd Street Groundwater Plume in McAllen, Hidalgo County, TX. Retrieved July 16, 2020, from https://www.tceq.texas.gov/remediation/sites/23rdstreet/23rd%20Street

TCEQ, Texas Commission on Environmental Quality, (Nov. 2019). “TRRP Protective Concentration Levels.” www.tceq.texas.gov/remediation/trrp/trrppcls.html.

Tchounwou, P. B., Yedjou, C. G., Patlolla, A. K., & Sutton, D. J. (2012). Heavy metal toxicity and the environment. *Experientia supplementum (2012)*, *101*, 133–164. https://doi.org/10.1007/978-3-7643-8340-4_6

Texas Demographic Center. (2019). "Demographic Characteristics, Trends, and Projections for Texas and the Rio Grande Valley." www.demographics.texas.gov/Resources/Presentations/OSD/2019/2019_02)22_UTRGV LegislativeInterns.pdf

Thomas, R., 2008. Practical guide to ICP-MS – a tutorial for beginners (2nd Ed) CRC Press, Boca Raton, Florida. 347p.

Thornton I. (1992). Sources and pathways of cadmium in the environment. *IARC scientific publications*, (118), 149–162.

TREBIEN, D. O. P., BORTOLON, L., TEDESCO, M. J., BISSANI, C. A., & CAMARGO, F. A. O. (2011). *Environmental Factors Affecting Chromium-Manganese Oxidation-Reduction Reactions in Soil. Pedosphere, 21(1), 84–89.* doi:10.1016/s1002-0160(10)60082-3

U.S. Composting Council. (2002). *Test Method for the Examination of Composting and Compost (TMECC) 04.12-B.* Raleigh, North Carolina.

USDA, ERS. Major Land Uses: Summary Tables. (2017, August 28). Retrieved December 12, 2019, from https://www.ers.usda.gov/data-products/major-land-uses.aspx.

Usman, A. R. A., Almutairi, A. A., Elmaghraby, S., & Al-Farraj, A. S. (2017). Levels, solid-phase fractions and sources of heavy metals at site received industrial effluents: a case study. Chemical Speciation & Bioavailability, 29(1), 78–88. doi:10.1080/09542299.2017.1324740

Wagatsuma, K., & Hirokawa, K. (1994). Analytical Performance of Inductively Coupled Plasma Emission Spectrometry Using Argon-Nitrogen Binary and Argon-Helium-Nitrogen Ternary Gas Mixture System. *Analytical Sciences*, *10*(3), 469–475. doi: 10.2116/analsci.10.469

Wang, M., & Zhang, H. (2018). Accumulation of Heavy Metals in Roadside Soil in Urban Area and the Related Impacting Factors. International journal of environmental research and public health, 15(6), 1064. doi:10.3390/ijerph15061064

Wilbur, Steven, 2007. https://www.agilent.com/cs/library/periodicals/Public/5989_6525_EN.pdf

Wilschefski, S. C., & Baxter, M. R. (2019). Inductively Coupled Plasma Mass Spectrometry: Introduction to Analytical Aspects. *The Clinical biochemist. Reviews*, *40*(3), 115–133. https://doi.org/10.33176/AACB-19-00024

Wilson, C. L., & Wilson, D. W. (2008). *Comprehensive Analytical Chemistry: Food Contaminants and Residue Analysis* (Vol. 51) (Y. Picó & D. Barceló, Eds.). Amsterdam: Elsevier. doi:10.1016/S0166-526X(08)00027-5

Wuana, R. A., & Okieimen, F. E. (2011). Heavy Metals in Contaminated Soils: A Review of Sources, Chemistry, Risks and Best Available Strategies for Remediation. ISRN Ecology, 2011, 1–20. doi: 10.5402/2011/402647

Wynne, B. (1994). The Impact of NAFTA on the U.S./Mexico Border Environment. *The Urban Lawyer, 26*(1), 11-30. Retrieved July 17, 2020, from www.jstor.org/stable/27894867

Yan, X., Zhang, F., Zeng, C., Zhang, M., Devkota, L. P., & Yao, T. (2012). Relationship between heavy metal concentrations in soils and grasses of roadside farmland in Nepal. International journal of environmental research and public health, 9(9), 3209-26. doi:10.3390/ijerph9093209

Zhang, Yanhao., Zhang, Haohan., Zhang, Zhibin., Liu, Chengying., Sun, Cuizhen., Zhang, Wen., Marhaba, Taha. (2018). pH Effect on Heavy Metal release from a Polluted Sediment. *Journal of Chemistry, 2018,* 1-7. Doi:10.1155/2018/7597640

Zwolak, A., Sarzyńska, M., Szpyrka, E. *et al.* (2019). Sources of Soil Pollution by Heavy Metals and Their Accumulation in Vegetables: a Review. *Water Air Soil Pollution* **230,** 164. https://doi.org/10.1007/s11270-019-4221-y

APPENDIX

APPENDIX

Table 2.8 ICP Raw Data in µg/l

Sample ID	As	Cd	Cr	Cu	Fe	Ni	Pb	Se	Zn
1	16.75	2.40	70.64	64.01	65633.41	66.18	55.52	0.56	240.68
2	35.32	2.08	58.03	76.40	55834.21	65.28	58.45	1.67	2084.08
3	3.49	1.96	60.26	177.48	59200.86	66.37	57.26	0.92	1089.70
4	8.00	2.04	58.27	61.86	55521.22	61.10	52.30	0.73	204.42
5	5.99	3.69	134.57	126.92	82133.78	151.47	130.18	2.36	655.05
6	13.11	3.92	127.28	108.38	84326.27	144.79	140.15	1.49	654.07
7	17.38	6.39	78.27	179.04	58263.74	189.30	90.95	0.61	2586.11
8	3.99	5.01	105.55	139.33	127168.74	138.22	115.60	3.17	884.48
9	5.35	3.17	106.96	267.46	98193.48	113.49	86.80	1.63	610.80
10	10.56	2.60	77.62	202.72	73005.85	72.63	74.23	1.03	490.45
11	12.90	3.92	151.84	145.24	155906.80	149.65	95.03	0.13	2339.46
12	28.80	2.53	265.16	362.66	82459.35	106.01	62.12	0.49	671.38
13	18.87	6.30	147.14	253.14	145452.53	136.59	244.95	3.01	2061.96
14	13.70	4.86	137.45	220.23	139910.08	135.97	184.01	1.61	1491.61
15	11.80	4.60	123.72	201.21	116399.21	105.74	119.28	2.02	629.92
16	16.24	4.28	143.63	216.73	156346.53	159.88	118.80	2.04	2987.25
17	17.61	3.43	145.48	165.32	160674.51	139.18	106.89	1.59	1790.82
18	9.41	3.37	150.34	205.55	163603.70	124.37	108.70	2.20	3397.12
19	11.94	4.15	117.19	228.35	87760.75	137.56	68.82	0.23	1566.26
20	24.72	2.46	72.77	149.50	66093.41	67.89	57.96	0.02	519.22
21	10.40	2.24	73.89	149.69	63826.62	54.36	55.34	0.13	419.16
22	10.70	2.37	95.93	126.21	92056.05	79.27	65.89	0.59	3638.63
23	32.79	1.91	68.68	183.58	65587.66	62.25	56.01	0.77	3554.30
24	6.63	2.72	79.13	175.74	78179.15	95.33	84.77	0.97	1667.14

25	16.71	2.66	85.46	189.70	81737.75	99.69	80.04	2.25	1919.05
26	19.93	3.22	73.98	141.63	65507.28	121.36	71.82	1.19	11663.06
27	6.69	2.66	89.67	109.99	86148.69	106.66	83.37	1.47	3299.10
28	14.82	2.57	90.78	140.70	86851.38	128.06	83.81	0.73	3069.85
29	30.41	2.60	85.35	109.21	84929.96	105.21	80.14	2.09	9283.61
30	9.13	2.37	78.81	169.06	77667.49	90.71	75.43	-0.11	499.10
31	7.53	2.99	88.70	128.69	78242.54	116.50	91.14	1.24	2428.92
32	16.38	2.68	93.14	138.51	77892.64	109.58	79.31	0.36	860.87
33	7.79	3.39	64.71	140.95	58720.95	80.93	87.21	0.97	4796.75
34	13.14	3.31	131.65	134.33	151253.25	138.87	112.91	0.72	527.22
35	13.80	3.82	124.30	128.18	147904.75	136.20	114.99	3.53	580.25
36	16.32	3.07	98.90	110.42	118107.89	101.99	85.84	0.83	443.74
37	10.50	3.41	128.64	148.24	152359.85	126.85	102.30	1.23	1656.91
38	9.60	3.33	119.68	126.11	139782.71	134.91	127.57	2.20	2751.32
39	15.02	3.66	99.18	114.26	92168.77	214.48	81.07	1.64	8297.91
40	9.87	3.33	142.63	117.83	143879.88	131.16	109.88	1.28	540.25
41	10.87	3.78	146.04	145.77	148835.22	121.43	104.79	2.37	1169.03
42	4.68	3.48	147.46	121.83	146844.12	125.51	103.91	2.25	3459.63
43	19.70	3.38	128.38	120.85	152635.88	127.82	105.08	5.49	649.37
44	11.16	4.31	160.53	176.59	173052.17	163.33	113.11	2.69	2708.97
45	13.99	4.69	154.88	135.65	178774.59	156.51	123.56	2.28	2892.45
46	4.76	4.10	145.23	138.84	172018.11	141.45	114.37	3.26	596.26
47	24.03	4.05	150.26	125.93	175445.85	145.38	117.35	2.82	616.29
48	15.83	4.10	134.40	245.53	92840.63	110.93	144.10	2.55	795.46
49	11.23	1.66	44.69	47.53	35152.32	37.97	42.47	0.72	226.46
50	20.21	2.00	60.01	39.55	50283.43	67.27	48.24	0.50	186.69
51	3.95	1.73	61.94	42.54	53168.22	59.82	47.12	0.50	177.64
52	17.19	2.48	68.64	52.15	61557.54	62.17	53.89	0.36	1800.18
53	31.35	2.05	68.77	53.77	59168.25	70.77	51.13	1.06	214.25
54	70.65	2.64	57.35	66.26	44053.57	44.74	47.14	1.64	417.27
55	15.64	2.50	63.12	59.75	43925.65	53.43	50.86	1.27	2686.55
56	25.40	2.70	57.24	72.51	44560.62	47.29	47.85	0.33	1687.06
57	9.39	2.10	47.70	55.64	39995.51	42.12	44.55	0.38	3193.63
58	5.18	2.10	47.12	42.94	40620.89	44.09	49.54	1.30	2588.30
59	9.86	1.76	47.94	44.32	41564.49	45.28	45.15	0.31	2123.89
60	16.13	1.69	51.09	39.77	43519.67	58.91	40.54	0.68	1057.33
61	25.37	2.11	58.10	51.94	47948.64	49.84	56.79	0.22	270.43

Table 2.9 AA Raw Data in µg/l

Sample ID	As	Cd	Cr	Cu	Fe	Ni	Pb	Se	Zn
1	38.67	0.319	98.72	44.59	74060	74.78	42.28	2.857	210
2	40.46	0.331	73.76	55.86	71540	78.21	53.53	2.902	205
3	37.73	0.07	73.24	127.3	73520	81.44	45.05	2.987	224
4	35.03	0.064	70.97	38.19	84080	71.02	42.66	2.652	785
5	115.8	1.016	134.1	77.04	61680	113.1	155.9	3.672	600
6	50.53	1.123	132.8	61.79	84220	101	177	3.391	2073
7	37.65	1.6	89.59	125.2	86150	187.1	95.84	3.17	462
8	69.14	0.905	110.6	96.16	144600	117.7	131	3.887	853
9	59.77	0.126	109.9	201.9	105900	107.4	98.5	3.224	571
10	33.9	0.067	106.3	128.5	78800	80.85	66.94	2.748	480
11	61.03	0.202	149.6	114.4	167200	135.7	112	3.178	828
12	46.69	1.279	210.1	280.7	43680	118.8	70.66	2.772	725
13	53	0.226	155.6	201.3	151200	133.2	307.4	3.14	1442
14	63.76	0.151	145.7	152.9	132700	138.2	223.4	3.224	997
15	61.51	0.122	134.4	130.8	149800	117.7	139.5	3.404	269
16	82.55	0.419	147.6	114.6	145200	137.3	129.6	3.441	1298
17	71.92	0.299	150.6	115.4	153900	123.2	124.9	3.45	511
18	63.21	0.238	131.6	210.5	141900	140.5	127.6	3.311	793
19	58.1	0.389	121.4	150.7	123500	169.4	48.73	2.261	384
20	47.38	0.036	81.49	47.35	76460	108.9	42.2	2.047	483
21	40.4	0.35	85.22	48.2	97900	74.53	42.91	1.212	416
22	71.08	0.333	104.2	56.18	106700	108.7	55.55	2.323	395
23	34.83	0.293	82.33	65.22	110700	101.1	38.93	2.074	353
24	48.57	0.394	141.5	92.32	83600	130.5	135.1	3.368	1220
25	50.68	0.046	97.22	57.69	107600	128.1	73.66	2.516	767
26	46.54	0.058	92.39	91.65	129100	166.5	88.87	2.696	546
27	43.97	0.03	96.23	72.66	147700	128.8	69.89	1.888	443
28	40.76	0.414	95.9	40.12	142500	149	62.6	1.964	2412
29	42.26	0.454	91.83	29.8	121700	125.8	57.92	2.097	365
30	46.09	0.046	85.76	100.8	91510	121.9	75.92	2.652	445
31	48.78	0.049	95.52	119.1	98140	149.7	96.46	2.564	474
32	41.7	0.05	94.21	72.33	107300	150.9	82.21	2.602	522
33	41.8	0.651	71.78	77.39	133600	117.5	86.17	2.503	780
34	102.7	0.174	125.4	103.8	163400	158.3	154.4	2.779	775
35	107.1	0.11	129.8	66.86	137200	150.9	135.5	2.598	501
36	90.39	0.601	109.6	59.36	121600	138.4	114.6	2.802	419
37	99.39	0.124	127.8	90.11	154800	151.9	133.1	2.524	529

38	95.13	0.685	121.1	74.74	139200	180.6	170.9	2.54	529
39	91.48	0.081	97.64	55.68	94500	245.1	101	2.59	436
40	119.6	0.121	124.6	65.88	137900	169.3	138.9	2.287	505
41	35.48	0.839	136	85.13	103100	103	132.1	2.248	7868
42	153.4	0.143	139.5	65.85	147500	161.2	127.5	1.995	710
43	105.1	0.197	127.8	73.58	154900	161.9	132.9	1.777	1049
44	117.6	0.379	146.1	75.05	35830	191.2	154.1	2.846	285
45	103.2	0.303	150.8	77.48	162000	173	154	2.116	647
46	112.1	0.324	140.8	83.18	175400	163.1	148.9	2.5	7763
47	112.8	0.31	151.5	72.95	171400	169	155.8	2.501	646
48	56.41	0.063	145.1	120	94920	178.6	162.5	2.081	2746
49	19.12	0.025	65.28	16.49	35150	73.4	32.13	2.102	200
50	23.43	0.057	80.12	11.25	69770	96.47	34.61	1.444	225
51	23.74	0.045	69.43	10.87	94410	97.41	41.27	1.561	213
52	22.51	0.046	80.29	23.8	112000	98.91	56.08	1.784	185
53	25.22	0.06	76.51	15.86	136900	110.9	53.17	1.515	198
54	17.12	0.024	63.85	19.22	56580	77.75	53.75	1.661	362
55	19.11	0.036	72.73	14.21	72300	83.13	55.25	1.25	295
56	18.26	0.435	64.1	20.74	66650	84.13	56.74	1.587	329
57	16.71	0.027	54.31	12.72	58490	71.76	48.75	1.626	298
58	21.11	0.042	51.15	13.63	65580	66.02	50.58	2.12	192
59	20.78	0.289	52.45	11.74	71430	68.92	56.17	7.597	184
60	53.03	0.043	56.46	10.91	96050	201.1	45.21	1.98	188
61	24.73	0.432	63.03	13.25	141000	84.44	63.14	2.651	264

Table 2.10 pXRF Raw Data (Wet) in µg/l

Sample ID	As	Cd	Cr	Cu	Fe	Ni	Pb	Se	Zn
1	40	100	50	50	150	60	40	20	40
2	40	100	40	50	150	60	40	20	40
3	50	100	50	50	150	70	40	20	40
4	40	100	30	50	160	60	40	20	40
5	70	250	100	60	240	90	50	30	60
6	80	310	110	60	250	90	60	30	60
7	60	110	50	50	160	70	40	20	50
8	60	210	80	60	220	90	50	30	50
9	60	130	60	50	190	70	40	20	50
10	50	110	50	50	170	60	40	20	50
11	60	160	80	60	200	100	50	30	50
12	60	120	60	50	180	60	40	20	50
13	70	140	60	60	210	80	40	20	50

14	70	140	70	50	170	90	50	30	50
15	70	140	70	60	190	80	50	20	50
16	60	180	70	50	180	100	50	30	50
17	60	180	80	60	200	100	50	30	50
18	70	170	70	50	160	100	50	30	50
19	50	100	40	60	170	60	40	20	40
20	60	100	40	50	150	60	40	20	40
21	50	110	50	50	130	70	50	30	40
22	40	90	50	40	180	40	30	20	40
23	60	130	40	50	160	70	40	20	40
24	60	130	50	40	150	70	50	30	40
25	70	160	60	60	180	110	50	30	50
26	70	120	60	50	150	80	50	30	50
27	50	130	60	40	130	90	60	30	40
28	50	110	50	50	140	80	50	20	40
29	50	100	40	50	170	60	40	20	40
30	50	130	50	50	180	70	40	20	40
31	60	130	50	50	190	60	40	20	50
32	60	130	50	50	160	70	40	20	40
33	60	130	50	40	150	70	50	30	40
34	70	160	70	60	180	110	50	30	50
35	60	130	60	60	170	100	50	30	50
36	60	140	70	60	180	90	50	20	50
37	60	140	70	60	180	100	50	30	50
38	70	140	70	60	190	100	50	30	50
39	60	120	60	50	170	80	50	20	50
40	60	140	60	60	180	100	50	30	50
41	60	140	70	50	170	110	50	30	50
42	60	140	60	70	190	90	50	30	50
43	60	150	70	60	190	100	50	30	50
44	70	180	80	60	200	110	50	30	50
45	70	180	80	60	220	100	50	30	50
46	70	180	80	60	200	110	50	30	50
47	70	180	80	60	200	100	50	30	50
48	80	120	60	60	170	90	50	30	60
49	40	110	50	40	130	60	50	30	40
50	40	100	30	50	160	60	40	20	40
51	40	100	40	50	150	60	40	20	40
52	40	100	30	60	180	60	40	20	40
53	40	100	40	60	160	70	40	20	40
54	50	110	40	40	140	70	50	30	40

55	40	100	40	50	150	60	40	20	40
56	50	100	50	40	130	60	40	20	40
57	40	110	50	40	120	60	50	30	40
58	40	100	30	50	160	50	40	20	40
59	40	100	50	50	140	60	50	20	40
60	40	100	50	50	140	60	50	20	40
61	50	100	50	50	140	60	50	20	40

Table 2.11 pxrf Raw Data (Dry) in µg/l

Sample ID	As	Cd	Cr	Cu	Fe	Ni	Pb	Se	Zn
1	40	100	40	50	170	70	40	20	40
2	40	110	30	50	170	70	40	20	40
3	40	110	50	50	160	60	40	20	40
4	40	120	40	50	170	70	50	20	40
5	70	250	100	60	230	90	50	30	60
6	80	310	120	60	280	90	50	30	60
7	60	120	60	50	180	70	40	20	50
8	80	240	90	60	240	100	50	30	60
9	60	150	60	60	200	80	50	20	50
10	50	110	50	50	170	60	40	20	50
11	60	170	70	60	200	100	50	30	50
12	70	120	60	60	210	60	40	20	70
13	80	150	60	60	200	90	50	30	60
14	70	150	70	60	200	90	50	30	50
15	70	160	70	60	190	80	50	20	60
16	60	210	80	50	190	110	60	30	50
17	60	190	80	60	220	100	50	30	50
18	70	180	70	60	220	90	50	30	50
19	50	110	50	50	170	70	50	20	40
20	50	100	50	50	160	60	40	20	40
21	50	100	50	50	150	70	40	20	40
22	50	120	50	50	170	80	50	20	40
23	50	110	40	50	160	70	40	20	40
24	60	130	60	60	190	80	40	20	50
25	60	120	50	50	180	80	50	20	50
26	60	120	60	60	180	70	40	20	50
27	60	110	50	50	170	70	40	20	40
28	50	110	50	60	170	70	40	20	40
29	50	110	50	60	170	70	40	20	40
30	50	130	60	50	180	70	50	20	50

31	60	140	60	50	170	70	50	20	50
32	6000	13000	60	60	190	70	50	20	50
33	70	130	60	50	180	70	50	20	50
34	60	160	70	60	190	110	50	30	50
35	60	140	60	60	170	100	50	30	50
36	60	140	60	50	170	100	50	30	50
37	60	140	60	60	190	100	50	30	50
38	60	150	60	60	180	110	50	30	50
39	60	130	60	50	190	80	50	20	50
40	60	140	60	60	190	100	50	30	50
41	60	140	60	60	200	100	50	30	50
42	60	140	60	60	190	100	50	30	50
43	60	160	70	60	200	100	50	30	50
44	70	200	80	90	210	110	50	30	50
45	70	190	80	60	230	100	50	20	50
46	70	190	80	50	180	120	60	30	50
47	70	190	80	60	210	110	50	30	60
48	70	130	60	60	190	80	50	20	50
49	40	100	30	50	150	50	40	20	40
50	40	100	40	50	170	70	40	20	40
51	40	100	40	50	160	70	40	20	40
52	40	100	40	50	170	70	40	20	40
53	40	100	40	50	170	70	40	20	40
54	60	100	40	50	160	60	50	20	40
55	50	100	40	50	170	60	40	20	40
56	50	100	40	50	160	60	40	20	40
57	50	100	40	50	170	60	40	20	40
58	40	110	50	50	150	60	40	20	40
59	40	100	40	50	160	60	40	20	40
60	40	100	50	50	150	60	40	20	40
61	40	110	50	40	150	70	50	20	40

Table 3.7 Sample Descriptions for Location, Zoning, Land Use, Distance, and Soil Conditions

Sample ID	***Location***	***GPS Coord.***	***Zoning***	***Land Use***	***Distance to main road (m)***	***Soil Conditions***				
						pH	% Sand	% Silt	% Clay	Soil Type
1	Peñitas	(26.330, -98.449)	U-IC	Community Garden	22.05	8	86	5	9	LS
2	Peñitas	(26.330, -98.449)	U-IC	Community Garden	18.77	7.83	88	4	8	LS
3	Peñitas	(26.330, -98.448)	U-IC	Community Garden	12.61	7.87	80	8	12	SL
4	Peñitas	(26.330, -98.449)	U-IC	Community Garden	10.51	8.03	88	4	8	LS
7	Donna	(26.158, -98.090)	U-IC	Community Garden	15.36	RB	90	4	6	LS
8	Las Milpas	(26.128, -98.192)	U-IC	Community Garden	12.08	7.81	96	1.8	2.2	S
9	Donna	(26.151, -98.116)	U-IC	Community Garden	17.63	8.23	88	4	8	LS
10	Donna	(26.152, -98.119)	U-IC	Community Garden	5.77	8.1	86	3	11	SL
11	Donna	(26.156, -98.090)	U-IC	Community Garden	31.99	7.92	82	8	10	SL
12	Donna	(26.151. -98.116)	U-IC	Community Garden	10.4	RB	91	1	8	LS
13	Donna	(26.151. -98.117)	U-IC	Community Garden	79.73	8.07	86	2	12	SL
14	Donna	(26.151. -98.117)	U-IC	Community Garden	76.06	RB	86	2	12	SL
16	Las Milpas	(26.139, -98.191)	U-IC	Community Garden	14.57	8	70	16	14	SL

17	Donna	(26.152, -98.091)	U-IC	Community Garden	22.83	7.83	72	6	22	SCL
18	Donna	(26.126, -98.192)	U-IC	Community Garden	1.38	7.9	90	8	2	LS
19	Edinburg	(26.349, -98.170)	IC	Citrus Grove	73.65	7.77	86	4	10	SL
20	Edinburg	(26.350, -98.170)	IC	Citrus Grove	29.46	7.64	88	4	8	LS
21	Edinburg	(26.351, -98.169)	IC	Citrus Grove	12.11	7.67	88	2	10	SL
22	Edinburg	(26.348, -98.172)	IC	Cotton Field	186	8.18	88	6	6	LS
23	Edinburg	(26.361, -98.206)	IC	Citrus Grove	214.46	7.89	90	2	8	LS
24	Palmview	(26.246, -98.363)	IC	Urban Farm	12.86	7.7	88	2	10	SL
25	Palmview	(26.246, -98.363)	IC	Urban Farm	21.51	7.65	90	4	6	LS
26	Palmview	(26.246, -98.363)	IC	Urban Farm	32.96	7.56	84	4	12	SL
27	Palmview	(26.246, -98.363)	IC	Urban Farm	33	7.53	80	8	12	SL
28	Palmview	(26.246, -98.363)	IC	Urban Farm	34.06	7.6	90	2	8	LS
29	Palmview	(26.246, -98.363)	IC	Urban Farm	35.09	7.7	88	6	6	LS
30	Palmview	(26.246, -98.363)	IC	Urban Farm	20.94	7.74	86	2	12	SL
31	Palmview	(26.246, -98.363)	IC	Urban Farm	19.99	7.75	90	2	8	LS
32	Palmview	(26.246, -98.363)	IC	Urban Farm	29.73	7.62	92	2	6	LS
33	Palmview	(26.246, -98.363)	IC	Urban Farm	21.94	7.9	84	2	14	SL

34	Mercedes	(26.230, -97.875)	IC	Corn Field	388.11	7.86	92	2	6	LS
35	Mercedes	(26.230, -97.876)	IC	Corn Field	314.21	8.03	82	4	14	SL
36	Mercedes	(26.228, -97.877)	IC	Corn Field	248.34	7.8	84	6	10	SL
37	Mercedes	(26.230, -97.878)	IC	Corn Field	142.35	7.96	88	10	2	SL
38	Mercedes	(26.230, -97.879)	IC	Corn Field	17.47	7.92	84	6	10	SL
39	Mercedes	(26.219, -97.877)	IC	Cattle Pasture	31.57	7.6	90	2	8	LS
40	Mercedes	(26.196, -97.878)	IC	Corn Field	x	8.12	72	6	22	SL
41	Mercedes	(26.195, -97.878)	IC	Corn Field	x	7.87	78	4	18	SCL
42	Mercedes	(26.194, -97.878)	IC	Corn Field	x	7.95	84	4	12	SL
43	Mercedes	(26.192, -97.877)	IC	Corn Field	x	7.93	80	6	14	SL
44	Mercedes	(26.190, -97.884)	IC	Sorghum Field	394.88	8.12	80	4	16	SL
45	Mercedes	(26.189, -97.884)	IC	Sorghum Field	316.65	7.97	58	18	24	SCL
46	Mercedes	(26.188, -97.884)	IC	Sorghum Field	185.27	7.9	84	4	12	SL
47	Mercedes	(26.188, -97.884)	IC	Sorghum Field	196.02	8.15	88	2	10	SL
48	San Isidro	(26.717, -98.455)	IC	Community Garden	44.02	7.84	84	4	12	SL
49	San Isidro	(26.718, -98.465)	IC	Community Garden	30.42	7.63	88	2	10	SL
50	San Isidro	(26.614, -98.541)	IC	Corn Field	9.99	7.86	96	2.8	1.2	LS
51	San Isidro	(26.614, -98.542)	IC	Corn field	85.3	7.91	82	8	10	SL

52	San Isidro	(26.614, -98.542)	IC	Corn Field	135.15	7.49	84	8	8	SL
53	San Isidro	(26.614, -98.542)	IC	Corn Field	176.12	7.62	80	10	10	SL
54	San Isidro	(26.616, -98.541)	IC	Farm Plot	20	7.36	88	2	10	SL
55	San Isidro	(26.617, -98.541)	IC	Farm Plot	20.99	7.86	88	6	6	SL
56	San Isidro	(26.617, -98.541)	IC	Farm Plot	36.34	7.78	88	4	8	SL
57	San Isidro	(26.617, -98.542)	IC	Farm Plot	37.24	7.65	92	2	6	LS
58	San Isidro	(26.603, -98.578)	IC	Farm Plot	12.02	7.96	84	8	8	SL
59	San Isidro	(26.603, -98.578)	IC	Farm Plot	29.5	7.86	88	2	10	SL
60	San Isidro	(26.604, -98.578)	IC	Farm Plot	37.66	7.97	88	4	8	LS
61	San Isidro	(26.604, -98.578)	IC	Farm Plot	47.91	7.77	86	6	8	SL

Table 3.8 ICP-MS Results per Sample

Sample ID	As	Cd	Cr	Cu	Fe	Ni	Pb	Se	Zn
1	16.75	2.4	70.64	64.01	65633.41	66.18	55.52	0.56	240.68
2	35.32	2.08	58.03	76.4	55834.21	65.28	58.45	1.67	2084.08
3	3.49	1.96	60.26	177.48	59200.86	66.37	57.26	0.92	1089.7
4	8	2.04	58.27	61.86	55521.22	61.1	52.3	0.73	204.42
7	17.38	6.39	78.27	179.04	58263.74	189.3	90.95	0.61	2586.11
8	3.99	5.01	105.55	139.33	127168.7	138.22	115.6	3.17	884.48
9	5.35	3.17	106.96	267.46	98193.48	113.49	86.8	1.63	610.8
10	10.56	2.6	77.62	202.72	73005.85	72.63	74.23	1.03	490.45
11	12.9	3.92	151.84	145.24	155906.8	149.65	95.03	0.13	2339.46
12	28.8	2.53	265.16	362.66	82459.35	106.01	62.12	0.49	671.38
13	18.87	6.3	147.14	253.14	145452.5	136.59	244.95	3.01	2061.96
14	13.7	4.86	137.45	220.23	139910.1	135.97	184.01	1.61	1491.61
16	16.24	4.28	143.63	216.73	156346.5	159.88	118.8	2.04	2987.25
17	17.61	3.43	145.48	165.32	160674.5	139.18	106.89	1.59	1790.82
18	9.41	3.37	150.34	205.55	163603.7	124.37	108.7	2.2	3397.12
19	11.94	4.15	117.19	228.35	87760.75	137.56	68.82	0.23	1566.26
20	24.72	2.46	72.77	149.5	66093.41	67.89	57.96	0.02	519.22
21	10.4	2.24	73.89	149.69	63826.62	54.36	55.34	0.13	419.16
22	10.7	2.37	95.93	126.21	92056.05	79.27	65.89	0.59	3638.63
23	32.79	1.91	68.68	183.58	65587.66	62.25	56.01	0.77	3554.3
24	6.63	2.72	79.13	175.74	78179.15	95.33	84.77	0.97	1667.14
25	16.71	2.66	85.46	189.7	81737.75	99.69	80.04	2.25	1919.05
26	19.93	3.22	73.98	141.63	65507.28	121.36	71.82	1.19	11663.06
27	6.69	2.66	89.67	109.99	86148.69	106.66	83.37	1.47	3299.1
28	14.82	2.57	90.78	140.7	86851.38	128.06	83.81	0.73	3069.85
29	30.41	2.6	85.35	109.21	84929.96	105.21	80.14	2.09	9283.61
30	9.13	2.37	78.81	169.06	77667.49	90.71	75.43	-0.11	499.1
31	7.53	2.99	88.7	128.69	78242.54	116.5	91.14	1.24	2428.92
32	16.38	2.68	93.14	138.51	77892.64	109.58	79.31	0.36	860.87
33	7.79	3.39	64.71	140.95	58720.95	80.93	87.21	0.97	4796.75
34	13.14	3.31	131.65	134.33	151253.3	138.87	112.91	0.72	527.22
35	13.8	3.82	124.3	128.18	147904.8	136.2	114.99	3.53	580.25
36	16.32	3.07	98.9	110.42	118107.9	101.99	85.84	0.83	443.74
37	10.5	3.41	128.64	148.24	152359.9	126.85	102.3	1.23	1656.91
38	9.6	3.33	119.68	126.11	139782.7	134.91	127.57	2.2	2751.32
39	15.02	3.66	99.18	114.26	92168.77	214.48	81.07	1.64	8297.91
40	9.87	3.33	142.63	117.83	143879.9	131.16	109.88	1.28	540.25

41	10.87	3.78	146.04	145.77	148835.2	121.43	104.79	2.37	1169.03
42	4.68	3.48	147.46	121.83	146844.1	125.51	103.91	2.25	3459.63
43	19.7	3.38	128.38	120.85	152635.9	127.82	105.08	5.49	649.37
44	11.16	4.31	160.53	176.59	173052.2	163.33	113.11	2.69	2708.97
45	13.99	4.69	154.88	135.65	178774.6	156.51	123.56	2.28	2892.45
46	4.76	4.1	145.23	138.84	172018.1	141.45	114.37	3.26	596.26
47	24.03	4.05	150.26	125.93	175445.9	145.38	117.35	2.82	616.29
48	15.83	4.1	134.4	245.53	92840.63	110.93	144.1	2.55	795.46
49	11.23	1.66	44.69	47.53	35152.32	37.97	42.47	0.72	226.46
50	20.21	2	60.01	39.55	50283.43	67.27	48.24	0.5	186.69
51	3.95	1.73	61.94	42.54	53168.22	59.82	47.12	0.5	177.64
52	17.19	2.48	68.64	52.15	61557.54	62.17	53.89	0.36	1800.18
53	31.35	2.05	68.77	53.77	59168.25	70.77	51.13	1.06	214.25
54	70.65	2.64	57.35	66.26	44053.57	44.74	47.14	1.64	417.27
55	15.64	2.5	63.12	59.75	43925.65	53.43	50.86	1.27	2686.55
56	25.4	2.7	57.24	72.51	44560.62	47.29	47.85	0.33	1687.06
57	9.39	2.1	47.7	55.64	39995.51	42.12	44.55	0.38	3193.63
58	5.18	2.1	47.12	42.94	40620.89	44.09	49.54	1.3	2588.3
59	9.86	1.76	47.94	44.32	41564.49	45.28	45.15	0.31	2123.89
60	16.13	1.69	51.09	39.77	43519.67	58.91	40.54	0.68	1057.33
61	25.37	2.11	58.1	51.94	47948.64	49.84	56.79	0.22	270.43

BIOGRAPHICAL SKETCH

Joy Youwakim is both a first generation Lebanese American and a southeast Texas native. She graduated from the University of Texas at Austin in 2018 with a B.A. in Economics with certificates in Environment and Sustainability and Food and Society. While studying at UT, she was introduced to the worlds of agriculture and food injustice through her calculus I professor, who was previously a Nebraskan corn farmer. The pair completed two research projects together, analyzing the drought resistant properties of sorghum in comparison to corn and the feasibility of growing produce atop closed landfills. This work led her to the discipline of soil contamination science. Joy is passionate about social justice and the accessibility of research to both the public and those who which to participate in it. She completed her Master of Science degree in Agricultural, Environmental, and Sustainability Sciences in August 2020. Joy can be contacted at jzyouwakim@gmail.com.